ZEOLITE SUPPORTED CdS/ZnO/Ag_3PO_4NANO-COMPOSITE: SYNTHESIS, CHARACTERIZATION AND PHOTOCATALYTIC ACTIVITY FOR THE DEGRADATION OF METHYLENE BLUE

MSc THESIS

GETACHEW ANJEJO CHEGASHA

JANUARY 2017

HARAMAYA UNIVERSITY, HARAMAYA

Zeolite Supported CdS/ZnO/Ag_3PO_4 Nano-Composite: Synthesis, Characterization and Photocatalytic Activity for the Degradation of Methylene Blue

A Thesis Submitted to the Department of Chemistry, Postgraduate Program Directorate, Haramaya University

In Partial Fulfillment of the Requirements for the Degree of
MASTER OF SCIENCE IN CHEMISTRY (INORGANIC CHEMISTRY)

GETACHEW ANJEJO CHEGASHA

January 2017
Haramaya University, Haramaya

HARAMAYA UNIVERSITY

POSTGRADUATE PROGRAM DIRECTORATE

As thesis research advisors, we here by certify that we have read and evaluated this thesis prepared, under our guidance by Getachew Anjejo entitled: Zeolite Supported CdS/ZnO/Ag_3PO_4 Nano-composite: Synthesis, Characterization and Photocatalytic Activity for the Degradation of Methylene Blue. We recommended as fulfilling the thesis requirement.

Abi Taddesse (PhD)	_____	_____
Major Advisor	Signature	Date
Tesfahun Kebede (PhD)	_____	_____
Co-Advisor	Signature	Date
Isabel Diaz (Prof.)	_____	_____
Co-Advisor	Signature	Date

As members of the board of examiners of the MSc thesis Open defense examination, we certify that we have read and evaluated the thesis prepared by Getachew Anjejo and examined the candidate. We recommended that the thesis be accepted as fulfilling the thesis requirement for the degree of Master of Science in Chemistry.

_____	_____	_____
Chairperson	Signature	Date
_____	_____	_____
Internal Examiner	Signature	Date
_____	_____	_____
External Examiner	Signature	Date

DEDICATION

This thesis is dedicated to my sister Aster Bekele and Abi Taddesse (PhD) for their great contributions in the success of my life.

STATEMENT OF THE AUTHOR

By my signature below, I declare and affirm that this Thesis is my own work. I have followed all ethical and principles of scholarship in the preparation and compilation of this Thesis. Any scholarly matter that is included in the Thesis has been given recognition through citation. This Thesis is submitted in partial fulfillment of the requirements for an MSc degree at the Haramaya University. The Thesis is deposited in the Haramaya University Library and is made available to borrowers under the rules of the Library. I solemnly declare that this Thesis has not been submitted to any other institution anywhere for the award of any academic degree, diploma, or certificate. Brief quotations from this Thesis may be made without special permission provided that accurate and complete acknowledgement of the source is made. Requests for permission for extended quotations from or reproduction of this Thesis in whole or in part may be granted by the Head of the Department or Director of Postgraduate Program Directorate when in his or her judgment the proposed use of the material is in the interest of scholarship. In all other instances, however, permission must be obtained from the author of the Thesis.

Name: Getachew Anjejo Signature: _____

Date: _____

Department: Chemistry

BIOGRAPHICAL SKETCH

The author was born on the 12th of April 1983 in SNNPR, Dawuro Zone, Gena Woreda at Wozo Kebele. He attended his elementary and secondary education in woldahane and Waka elementary and secondary schools respectively. Later, he joined Hawassa Teachers' Education College and graduated with Diploma in teaching chemistry in 2004. He was then assigned by the Educational Beruea of SNNPR in Issera Balle preparatory secondary school. Then he joined Mizan Tepi University in 2007 to summer in service degree program in Teaching Education and received B.Ed. degree in chemistry in 2010. He continued his service with B.Ed until he joined the Postgraduate Program at Haramaya University to pursue MSc program in Inorganic Chemistry in September 2013.

ACKNOWLEDGEMENTS

The author would like to thank Abi Taddesse (PhD) for providing financial support for carrying out this research work, Isabel Diaz (Prof.) for XRD, SEM-EDS and UV-Vis measurement that is highly appreciable and Tesfahun Kebede (PhD) for his constructive comments and suggestions.

The author also would like to Thank Chemistry Department of AAU for the FT-IR and PL characterization of his samples. Special thanks should go to Mr. Solomon Bezabih for running the PL spectra of the as-synthesized samples.

The author would like to acknowledge Mr.Fituma Deriba for providing instrumentation facility.

Last but not least, the Department of Chemistry of Haramaya University deserves acknowledgment for hosting me in this postgraduate program.

ACRONOMYS AND ABBREVIATIONS

AAS	Atomic absorption spectroscopy
FT-IR	Fourier Transform Infrared
SEM	Scanning Electron Microscopy
UV-Vis	Ultra Violet and Visible light
XRD	X-ray Diffraction
PL	Photoluminescence
CB	Conduction band
VB	Valence band

TABLES OF CONTENTS

LIST OF TABLES

LIST OF TABLES IN THE APPENDIX

Appendix Table **Page**

LIST OF FIGURE

LIST OF FIGURES IN THE APPENDIX

Zeolite Supported CdS /ZnO/Ag_3PO_4 Nano-Composite: Synthesis, Characterization and Photo catalytic Activity for the Degradation of Methylene Blue

ABSTRACT

The single, binary and ternary systems nano-materials were synthesized by co-precipitation method. The zeolite supported terray nanocompsotes were prepared by impregnation method using synthetic zeolite as the supporting material. The structures, compositions, surface functional groups and band gap energies of the composites were studied using X ray diffraction (XRD), FTIR, PL, AAS, and UV–Vis diffuse reflectance spectroscopic techniques. Photocatalytic degradation activities of the nano-composites under visible light irradiation were evaluated on aqueous solution of a model pollutant Methylene Blue dye solution as well as on a real sewage sample solution collected from Hawassa Textile Industry. Results suggested that the zeolite supported ternary nano-composite photocatalyst exhibited a relatively higher efficiency on the photodegradation of both Methyenel blue (MB) 92.57% and real sewage sample solutions 73.24%.. The improved photodegradation efficiency in the visible region of the supported nanocomposite is due to the sorption or ion exchange ability of the zeolite material. The reusability of this photocatalyst was tested and only an 18 % decrement was observed after four cyclic run.

Keywords: *Nano-composite, Ternary system, Immobilization, Photocatalysis, Zeolites, Heterojunctions*

1. INTRODUCTION

The textile industry is the largest consumer of dye stuffs. During the coloration process a large percentage of the synthetic dye does not bind and is lost to the waste stream (Weber and Adams, 1995).The effluent from textile industries thus carries a large number of dyes and other additives which are added during the coloring process (Wang *et al.,* 2002). The dyes are generally stable to light, oxidizing agents and heat, and their presence in wastewaters offers considerable resistance to their biodegradation, and thus upsetting aquatic life (Robinson *et al.,*2001; Aksu, 2005).These are difficult to remove in conventional water treatment procedures and can be transported easily through sewers and rivers because they are designed to have high water solubility. They may also undergo degradation to form products that are highly toxic and carcinogenic. Thus dyes are a potential hazard to living organisms. It is hence important to safeguard the environment from such contaminants.

Various processes such as precipitation, adsorption, air stripping, flocculation, reverse osmosis and ultra filtration can be used for color removal from textile effluents. However, these techniques are non-destructive since they only transfer the non-biodegradable matter into sludge, giving rise to new type of pollution, which needs further treatment. Stopping such chemical dye waste from polluting rivers, environment and waterways could be much easier, due to recyclable metal oxide cleaning system developed by nanotechnology. Among many strategies, photocatalysis is regarded as the most viable one, especially for treatment of contaminants, due to its usage of sunlight to decompose organic pollutants (Bahnemann,2004; Zhao *et al.,*2005;Gaya *et al.,* 2008). Photocatalysts absorb light energy and make this energy available as chemical energy. Photo excited electrons have two possibilities: loose energy and fall back to its original valence energy level or migration to a slightly lower energy level on another proximate molecule (Zhou *et al.,* 2010). This electron-hole separation will then start the desired redox reactions, and once they are completed, the photocatalyst will be back in its original state(Xiang *et al.,* 2012).In order to prevent the recombination of the photo induced e^-/h^+ pairs, one usually can improve the crystallinity, decrease the particles size, and load catalyst such as Pt, Pd, NiO, and RuO_2 on the surface of photocatalyst.

The higher crystallinity results in fewer defects which act as the recombination center of photo induced e-/h+ pairs. The recombination of excited charges decreases the photocatalytic activity.

On the other hand, the smaller size of the particle, the shorter distance that the photo induced e-/h+ pairs must migrate to the reaction sites on the surface, which decrease the recombination probability. In the case of co-catalyst, a heterojunction is built between the host semiconductor and the co-catalyst and subsequently an internal electric field is formed, which facilitates the separation of the photo excited carriers. Furthermore, these co-catalysts show better conductivity, lower over potential, and higher catalytic activity than the host semiconductors. Accordingly, they usually act as ideal active sites for photocatalytic reactions.

Semiconductor photocatalysis, as green technology, has received a great deal of research interest due to its universal applications especially in utilization of solar energy, environmental purification (nonselective process), and selective organic transformations to fine chemicals. It is also a versatile, cost effective and eco-friendly treatment technique for the destruction of organic pollutants in water (Kim, 2006). Among the materials being used, Nano-particles ZnO has been widely used as a photocatalyst, owing to its high activity, low cost, and environmentally friendly feature (Xu *et al.,* 2011). However, the photocatalytic activity of ZnO is limited to irradiation wavelengths below 387 nm because ZnO semiconductor has a wide band-gap of about 3.2 eV and only 3–5% of the whole solar energy is effectively utilized, while 43% of the visible light is open to exploit. On the other hand, the rapid recombination of photo generated electron–hole pairs on ZnO particles inevitably hinders the outward diffusion of the charge carriers. Therefore, the photo catalyzed degradation occurring at the semiconductor/liquid interface is prohibited, which is another vital limiting factor to the photocatalytic efficiency. In order to overcome the mentioned two drawbacks of ZnO, plenty of methods such as doping with metal and nonmetal elements, combination with other semiconductor materials, sensitization by organo metallic dye molecules, etc (Zhao *et al.,* 2008; Zhao *et al.,* 2010; Lee *et al.,* 2012; Zou *et al.,* 2013) have been applied to enhance the charge separation and improve the visible light response of ZnO based photocatalysts. Among them, a good strategy is coupling of two or more semiconductors to form composite photocatalysts, because it has been reported that if two or more semiconductors are properly integrated into one system, this system can be expected to achieve high photocatalytic activity (Kamat, 1993). For example, the SnO_2/ZnO, TiO_2/ZnO (Zhang *et al.,* 2008), WO_3/ZnO composite hetero structures appear to be very efficient for the photo decomposition of organic dyes compared to ZnO alone (Yu *et al.,* 2011).

The narrow band-gap semiconductors usually act as visible-light sensitizes, and some of the photo generated electrons or holes excited by visible light irradiation will then transfer to ZnO. In most of the composites, the conduction band (CB) level of the sensitizer is located relatively higher than that of ZnO. Hence the electrons photo generated by the sensitizer is transferred to the CB of ZnO, and these energetic electrons can initiate many reduction reactions. Such systems are classified as "Type-A hetero-junction", which will be eligible for the reduction reaction or partial decomposition of organic pollutants (Bessekhouad *et al*., 2006). However, CO_2 evolution resulting from complete oxidation of organic pollutants will be slow, due to the unavailability of the •OH radicals on the ZnO surface.

Contrarily, if the valence band (VB) level of the sensitizer is located lower than that of ZnO , the visible-light sensitization can induce the hole-transfer from the sensitizer to ZnO. As a result, holes can be generated in the VB of ZnO, initiating in turn various oxidation reactions. Considering the powerful oxidative ability of the holes in the VB of ZnO, efficient and complete oxidation of organic compounds is expected to this system denoted as "Type-B hetero-junction" under visible-light. And it is evidenced in the recent literatures as a possible way to develop new visible-light-responsive photocatalysts with high activity (Kim *et al*., 2011)**.**

To further improve the photocatalytic performance, ternary nano-composite materials systems have also received particular attention. For instance, Kim *et al.,*(2011) reported the synthesis of $CdS/TiO_2/WO_3$ ternary hybrid systems as new photoactive composites and found that the ternary hybrid exhibited much higher photocatalytic activity than that of CdS alone or binary hybrids. In another study, Lin *et al.,* (2009) prepared CdS nanoparticles/ZnO shell/TiO_2 nanotube (NT) arrays for water splitting and found that the conversion efficiency increased from 0.39% to 1.30%. Furthermore, Chen *et al.,* (2011) described a new method to form a ZnO energy barrier layer between TiO_2 NTs and CdS quantum dots, which exhibited improved efficiency of the quantum dots-sensitized solar cells. The ternary systems described above however didn't take into account the possible advantages to be exploited by designing ternary systems combining "A-B hetero junctions". We hypothesized that the combined A-B heterojunctions could exhibit better photocatalytic activity than the respective A-type and B-type hetero junctions. This work also focuses on supporting the as-synthesized A-B heterojunctions onto zeolite to improve the recyclability of the nano-materials.

Some problems such as the way of separating the Nano-particles and the low efficiency of photocatalyst reactions in aqueous solutions can limit the usefulness of the Nano-particles. Recently, many studies have been carried out in searching for an appropriate substrate for photocatalyst particles to be supported in order to improve the efficiency of photocatalyst recovery (Tao *et al.,* 2006; Hisanaga and Tanaka, 2002; Shankar *et al.,* 2006). Out of several substrates, zeolite seems more appropriate due to their unique structure, uniformed pores and channels and excellent ability in attaching to photocatalyst (Huang *et al.,*2008; Takeuchi *et al.,* 2009). Many researchers have firmly confirmed working with synthetic zeolites (Kim and Yoon, 2001; Anandan and Yoon, 2003; Tao *et al.,* 2006; Haileyesus Tedla *et al.,* 2015).

Zeolite with its well defined structure and micro-porous cavities work as a good candidate for nano-particles support and hosting (Bercoff *et al*., 2009). The interaction of nano-particles in both form of metal and metal oxide with zeolite has opened a new window of applications such as sensors, electronics, magnetic and photcatalytic applications (Bercoff *et al.,* 2009). Their adsorption capacities help in attracting contaminants to the surface and thus enhance the efficiency of the dispersed nano-particles. Therefore, the purpose of the present work is to synthesize and study the photocatalytic activities of the zeolite supported CdS/ZnO/Ag_3PO_4 nano-composites for Methylene Blue and real sewage sample collected from Hawassa Textile Industry degradation under visible light illumination.

General objective:

To assess the photo catalytic performance of zeolite supported CdS/ZnO/Ag_3PO_4 nanocomposite

Specific objectives:

- ✓ To synthesize nanosized ZnO, CdS/ZnO, Ag_3PO_4/ZnO, CdS/ZnO/Ag_3PO_4 and zeolite-supported CdS/ZnO/Ag_3PO_4 nanocomposite.
- ✓ To characterize the as-synthesized material using various techniques such as AAS, XRD, SEM-EDX, FITR, PL and UV-Vis.
- ✓ To evaluate the effect of operating conditions (parameters) on the photocatalytic activity of zeolite supported CdS/ZnO/Ag_3PO_4 nanocomposite.
- ✓ To evaluate the recyclability of the zeolite-supported CdS/ZnO/Ag_3PO_4 nanocomposite.

2. LETRETURE REVIEW

2.1. Nanomaterials

Nanocomposites are materials with at least in one dimension in which at the nanometer range ($1nm=10^{-9}m$).Nowadays Nano-materials are great interest from research point of view because the properties of the materials change drastically when the particle size reaches to nano meter range. As the size of the material becomes smaller, the band gap becomes larger there by changing the optical and electrical properties of the material and making the material suitable for newer applications and devices. Further, the use of nano-particles exhibit higher photocatalytic activity than their bulk counter parts by increasing their surface area and porosity.

Nano-composite material have emerged as suitable to overcome limitations of micro and monolit hic,while posing preparation related to the control of elemental compositions and stoicchiometry nanocluster phase. They are to be the materials of 21^{st}century in the view of possessing design uniqueness and property combinations that are not found in conventional composites. It has been reported that the changes in particle properties can be observed when the particle size is less than a particular level, called, the critical size (Kamigaito *et al.,*1991). As the dimensions reach the nano meter level, interactions at phase interfaces become largely improved, and this is important to enhance materials properties. In this context, the surface area to volume ratio of reinforcement materials employed in the preparation of Nano-composites is crucial to the understanding of their structure properties relationships. Now, several researchers have focused on metal oxides nano-particles and their composites for their high BET surface areas and fast kinetics when subjecting to the treatment of organic pollutants in water and air. The general understanding of these properties and application is very important.

Nano-particles of semiconductors have a great potential as water purification catalysis and redox active media due to their large surfaces, and their size and shape dependant optical, electronic and catalytic properties (Obare andMeyer *et al*., 2004). Environmental pollution had an influence on human survival and development. Nano-particles are of interest because of their high reactivity due to the large surface area to volume ratio. It was observed that nano-materials displayed significantly different properties at nanometer sizes as compared to the properties of

the same material in bulk and that the properties of the materials are size and shape-dependent at nano scale range (Caruso, 2001). The large surface area of small-sized particles is expected to be beneficial for photocatalytic reactions that mostly occur on the surface of the catalysts (Kama *et al*., 1993**).**

2.2. Photocatalysts

Photocatalysts are molecules that are activated using natural light and work to improve how well a reaction would normally run (Huang *et al*., 2010). Photocatalysis is a catalytic reaction involving light absorption by a catalyst or a substrate. Heterogeneous photocatalysis has emerged as an important destructive technology leading to the total mineralization of most of the organic pollutants including organic reactive dyes.

Nano-science andtechnology have attracted significant attention due to their potential application in various fields (Xi *et al.,* 2004). With the development of industry and economy, environmental problem become more and more serious day by day. Due to certain man made activities, numerous hazardous compounds are introduced into the environment which is a concerning matter for monitoring agencies and regulation authorities. Photocatalysis has been regarded as the most viable technology to solve this problem. Various photocatalysts, especially metal oxide photocatalysts such as TiO_2, SnO_2 and ZnO have attracted extensive attention for the degradation of organic pollutants in water and air under UV irradiation (Fotou and Pratsinis, 1996; Curridal *et al.,* 2003; Chakrabarti *et al.,* 2004; Hong *e*t *al.,* 2006).

Photocatalytic technology has become a major way for dominating environmental pollution. In the past few decades, the searching of various suitable visible-light-driven photocatalysts for splitting of water and degradation of organic contaminants is one of the significant tactics for solving energy crisis, global environment pollution and climate change (Walte *et al.*,2010). Since 1972, TiO_2, ZnO, WO_3 and other wide band gap semiconductor photocatalysts had been widely used as a conventional functional material for clean energy and environmental protection (Han *et al.,* 2009), in photocatalytic degradation of various pollutants (Liu, 2008; Yang *et al***.,** 2012), the destruction of bacteria (Hu *et al*., 2012**)** and catalysis by lots of research groups.The above-mentioned nano structured semiconductors can largely promote photocatalytic activity because

of their unique properties derived from low dimensionality and quantum confinement effect. Indeed, the nano-sized materials with high surface areas exhibited enhanced photo activities, because the photo-generated electron–hole pairs could move effectively to the surface to increase the number of active sites, and therefore the photocatalytic reaction would be enhanced markedly. On the other hand, the nano scaled structure-induced quantum size effect will also promote the photocatalytic activity.

Photocatalysis has emerged as a promising technique owing to its valuable applications in environmental purification. With the demand of building effective Photocatalyst materials, semiconductor investigation experienced developing process from simple chemical modification to complicated morphology design. Environmental pollutants such as dyes, phenols, pesticides, etc. which discharged by industries or by certain man made activities have adverse effect and causes water pollution, environmental contamination and big threat to human health and aquatic ecosystem due to their toxicity, carcinogenicity and hazardous effect (Constapel *et al.,* 2009). Photocatalyst plays an important role in the environmental safety by photocatalytic degradation of pollutants. In the last years, much research efforts have been focused on finding an active catalyst suitable for detoxification of these pollutants. Photocatalysts have recently been the subject of numerous studies and in particular with a view to applications in environmental protection, *(*Elahifard *et al.,* 2007; Ewais *et al.,* 2008).These molecules have been studied for uses in producing clean energy, namely for water splitting, as a way to break down pollutants, and for self-cleaning products (Aveyard *et al.,* 2005; Liu *et al* 2011). There has been utilization of advanced oxidation processes (AOPs) for the complete destruction of dyes. AOPs are based on generation of reactive species such as hydroxyl radicals that oxidizes a broad range of organic pollutants quickly and non-selectively. AOPsinclude photocatalysis systems such as combination of semiconductors and light, and semiconductor and oxidants.Recently considerable attention has been focused to develop semiconducting metal oxide for safety of environment by environmentalist and scientific community.Some metal oxide semiconductors such as Fe_2O_3, ZnO, TiO_2, WO_3, Cu_2O, and SnO_2 are being used as photocatalysts (Kansal *et al.,* 2007). These nanostructures were applied for catalytic and sensing application and demonstrated good degradation and sensing properties. To overcome limitation, several attempts have been made to evaluate the photocatalytic activity using suitable supports.

Immobilizing photocatalysts on appropriate supports is beneficial for wastewater treatment by photocatalysts. Small sized and well-distributed Ag_3PO_4 particles immobilized on flaky layered double hydroxide (FLDH) together with the strong adsorption of dye enhanced its photocatalytic properties demonstrated by (Chatterjee *et al*.,2005) .Coreshell Nano-composites, including multi-phase semiconductors, metal semiconductors and metal metal nanocomposites, have been the subject of extensive research, because of their tunable surface properties, enhanced optical, electronic, catalytic properties and their potential applications in many areas such as microelectronics, optoelectronics, optical devices, and catalysis in the past decades.

2.3. Photocatalytic principle

Photo reactions do not occur on illumination with light alone. These reactions often require the use of a photocatalyst. In the case of semiconductor material the role of photons is to generate electron (e^-)-hole (h^+) pairs that take part in subsequent redox reactions with the surface adsorbed molecules to yield the ultimate products.When light of a certain wavelength falls on a semiconductor and its energy is more than or equal to the band gap energy of the semiconductor, electrons would be excited from the valence band to the conduction band of the semiconductor and holes would be left in the valence band. These electrons and holes undergo subsequent oxidation and reduction reactions with any species, which are adsorbed on the surface of the semiconductor to give the necessary products (Chatterjee *et al*., 2005). The positive hole oxidizes either the pollutants directly or water to produce hydroxyl radical ($HO^{\cdot}$), whereas the electron in the conduction band reduce the oxygen adsorbed on the photocatalyst (Ahmed *et al*., 2010).

Oxidative reaction:

$$h^+_{(VB)} + \text{organic dye} \longrightarrow (\text{intermediates}) \longrightarrow CO_2 + H_2O$$

$$h^+ + H_2O \longrightarrow OH^- + H^+$$

Reductive reaction:

$$e^-_{(CB)} + O_2 \longrightarrow O_2^-$$

$$O_2^- + H + HO_2^{\cdot} \longrightarrow OH^{\cdot} + \text{Organic dye} \longrightarrow (\text{intermediates}) \longrightarrow CO_2 + H_2O$$

In the degradation of organic pollutants, the hydroxyl radical generated from the oxidation of adsorbed water is the primary oxidant, and the oxygen present react with electron at the conduction band to form peroxide radicals followed by a number of steps forming H_2O or OH radical thus prevent the recombination of an electron hole pair. The hydroxyl radical attacks organic compounds resulting in various reaction intermediates depending on the nature of the compound. The resulting intermediates further react with hydroxyl radical to produce final degradation products as carbon dioxide and water.

Excited-state conduction-band electrons and valence-band holes can recombine and dissipate the input energy as heat, get trapped in meta stable surface states, or react with electron donors and electron acceptors adsorbed on the semiconductor surface or within the surrounding electrical double layer of the charged particles. In the absence of suitable electron and hole separation forces, the stored energy is dissipated within a few nanoseconds in the recombination process. If a suitable scavenger or surface defect state is available to trap the electron or hole, recombination is prevented/reduced and subsequent redox reactions may occur. Photocatalysis has been applied successfully for the removal or degradation of pollutants, or used as pretreatment to convert pollutants into shorter-chain compounds that can then be treated by conventional or biological methods (Gogate *et al.,* 2004; Anjaneyulu *et al*., 2005). The efficacy of photocatalysis depends on the concentration of reactive free radicals, the most important of which is the hydroxyl radical ($OH^{\cdot}$) (Gogate *et al.,* 2004; Catalkaya *et al.,* 2007). Free radical species are atoms or molecules that are capable of independent existence and possess one or more unpaired electrons such as superoxide radicals ($O^{\cdot}_2$), hydroperoxyl radical ($HOO^{\cdot}$), and hydroxyl radical ($OH^{\cdot}$) (Gome *et al*., 2005). Among these various radicals, the hydroxyl radical is thought to play a central role in photocatalysis for wastewater treatment (Tai *et al*., 2002).

2.4. Semiconductors

The semiconductors are substances with electronic structure characterized by a filled valence band and an empty conduction band. The energy difference between the conduction band and the valence band is called band gap energy. Semiconducting nano-particles are a special class of

nanostructure materials that are under intense investigation due to their unique optical and electronic properties.

A semiconductor is a substance, usually a solid chemical element or compound that can conduct electricity under some conditions but not others, making it a good medium for the control of electrical current. Its conductance varies depending on the current or voltage applied to a control electrode, or on the intensity of irradiation by infrared, visible light, ultraviolet (UV), or X rays. The specific properties of a semiconductor depend on the impurities, or dopant, added to it. A hole has a positive electric charge, equal and opposite to the charge on an electron. In a semiconductor material, the flow of holes occurs in a direction opposite to the flow of electrons. Semiconductor photocatalysts are semiconductors which are able cause or accelerate chemical reactions upon light absorption, typically sunlight. By utilizing the energy of absorbed photons, photocatalysts can be optimized to carry out a wide variety of important chemical processes such as environmental remediation - the destruction of organic pollutants for water or air purification, solar fuels production - production of fuels, H_2 from water or methane/methanol from CO_2. Semiconductors can be used in photocatalysis as particle dispersions or in photoelectrochemical mode. Several hybrid structures have been envisaged to improve photocatalytic performance of semiconductors such as semiconductor-semiconductor, semiconductor-metal, semiconductor-Reduced Graphene Oxide (RGO) nano-assemblies.

2.5. Properties of ZnO

Zinc oxide (ZnO) is an important industrial material, because it has an inorganic and semiconducting material with inherent properties that share its structure as wurtzite (Mishra *et al*., 2012). ZnO nano-composite has attracted interest because of its optical properties. These particles are transparent to visible light, but they absorb UV-light. ZnO has attracted intensive research effort for its unique properties and versatile applications in transparent electronics, chemical sensors, and spin electronics (Ushio *et al*., 1994; Harima and Könenkamp, 2004; Lee *et al*., 2005).ZnO is soluble in acid and alkalis, but nearly soluble in water.In nature, it occurs as mineral zincites.Crystalline zinc oxides exhibit piezoelectric behavior. When heated with carbon the oxides converted into zinc.It has different applications such as medical, chemical and biosensor. Due to its high isoelectric points (9.5), biocompatibility and fast electron transfer,

interest has recently been focused onto the applications of ZnO in biosensing. ZnO is reactive towards both acids and base, so it is considered as an amphoteric oxide. Nano sized ZnO has been widely used as a catalyst (Kamat *et al.,* 2002 ; Chauhan *et al .,* 2011), gas sensor (Lin *et al.,* 1998 ; Xu *et al*., 2000) active filler for rubber and plastic, UV absorber in cosmetics and antivirus agent in coating and has more potential application in building functional electronic devices with special architecture and distinctive optoelectronic properties(Chen *et al.,*2003; Li and Wu , 2003). It exhibits direct and wide band gap, strong sensitivity of surface to the presence of adsorbed species and large excitation band energy. Partial list of above properties distinguishes it from other semiconductors or oxides and make useful for applications.

2.6. ZnO Semiconductor

ZnO semiconductor is known to be the best photocatalyst for the degradation of several environmental contaminates. However, ZnO semiconductor absorbs large fraction of solar UV light. The basis of photocatalysis is the photo excitation of a semiconductor solid as a result of the absorption of radiation. In many studies, extensive investigations have been concentrated on the design and synthesis of binary semiconductor metal oxides such as TiO_2/ZnO, Ag_3PO4/ZnO and CdS/ZnO nanocomposite materials to improve the photocatalytic efficiency in water purification and degradation of organic pollutants (Janitabar *et al.,* 2009; Bai *et al.,* 2010). Therefore, various ways have been adopted to improve the ZnO semiconductor utilization of the visible light (Zhong *et al.,* 2012). The improvement is largely attributed to the formation of a potential gradient at the interface. However, only a few systems utilizing hole-transfer between the sensitizer and ZnO have been reported (Xu *et al*., 2000), owing to the scarcity of suitable sensitizers.

2.7. ZnO based Heterojunctions

ZnO is a widely used catalyst to oxidize or reduce the organic pollutants in industrial wastewater as it is non-toxic, inexpensive, stable and photoactive (Pare *et al.,* 2011). ZnO, as it is, can be excited only by UV light due to its large band gap energy of 3.2 eV. However, photocatalysis using visiblelight has been receiving increased attention hence, modification of ZnO is necessary for its enhanced response to visible light (Chatterjee *et al.,* 2005).

There are many methods of modifying ZnO, such as doping and photo sensitization. Semiconductor sensitization is a technique used to reduce its band gap energy requirements. Photosensitized degradation process, assisted by visible light, involves the initial excitation of the surface adsorbed dye followed by the charge injection to the conduction band of the semiconductor which results in the photocatalytic degradation reaction. Semiconductor photo-sensitizer molecules adsorbed on the surface extend the range of excitation energies of the semiconductor into visible region. CdS and Ag_3PO_4 are considered to be the most suitable visible sensitizer for ZnO because the lattice structure of CdS and Ag_3PO_4 are same as that of ZnO, the band gap lies in the visible range and the CdS forms a type-A hetero- junction with ZnO which facilitates a very fast, inter band charge transfer from CdS to ZnO while Ag_3PO_4 form Type-B hetero-junction.

It has been reported that the CB and VB edge potential of Ag_3PO_4 is 0.45 eV and 2.9 eV (vs. NHE), respectively (Ouyang *et al*., 2011). The CB potential of Ag_3PO_4 is lower than that of ZnO with 2.6 eV and some of the electrons in the CB of ZnO can be transferred to that of the sensitizer, (Ag_3PO_4), and consequently the holes generated in the VB of ZnO can initiate photocatalytic oxidation reactions. The $^{\cdot}OH$ radicals generated in the VB of ZnO play the primary role in the visible-light photocatalytic degradation of pollutants. So Ag_3PO_4 is considered to be an appropriate sensitizer to improve photocatalytic activity in the Ag_3PO_4/ZnO system, in which ZnO works as a substrate, while the role of Ag_3PO_4 is a sensitizer absorbing visible light(Ouyang *et al*., 2011).

$$(ZnO)\ VB\quad h^+ + H_2O \longrightarrow OH^{\cdot} + H^+$$

$$h^+ + OH^- \longrightarrow OH^{\cdot}$$

$$CB\ e^- + O_2 \longrightarrow {}^{\cdot}O^-_2$$

$$e^- + O_2 + H^+ \longrightarrow {}^{\cdot}H$$

$$2e^- + O_2 + 2H^+ \longrightarrow H_2O_2^{\cdot}$$

$$e^- + H_2O_2 \longrightarrow {}^{\cdot}OH + OH^-$$

In another hand CB potential of CdS is higher than that of ZnO. When the Ag_3PO_4/ZnO photo-catalyst is irradiated by solar light photo generated electrons are injected from the CB of the photo excited CdS into the CB of ZnO, leading to a high concentration of electrons in the CB of

ZnO. In this way, the charge separation is achieved. Meanwhile, the holes generated on CdS VB are not transferred to the corresponding band of ZnO due to the CdS VB being more cathodic than that of ZnO. Consequently, a high concentration of holes in the VB of the CdS nanoparticles can be obtained. Holes in CdS could potentially react with water adhering to the surface of the CdS nanoparticles to form highly reactive hydroxyl radicals (OH^-). It is possible that the holes themselves directly oxidized the organic molecules.

Subsequently, the CB electrons (e^-) accumulated on the surface of ZnO are then scavenged by dissolved oxygen molecules in water to yield highly oxidative species such as superoxide radical anion (O_2^-) and hydroxyl radical ($OH^\cdot$), which can decompose organic pollutants effectively.

2.8. Immobilization of nanomaterials

Application of support for the nano photocatalyst maintains the dispersion of the nanoparticle and prevents agglomeration and sintering (Li *et al.,* 2008; Qiu *et al.,*2011). Also, support increases the photocatalytic activity by enhancing charge separation (high electric conductivity supports) or the adsorption of organic molecules (Vu *et al.,* 2013). Generally support/magnetic coating is used to immobilize the nanocatalyst so that the reusability of nanocatalyst can be achieved (Lucas *et al.,*2013; Shao *et al.,* 2013), and also supports help the adsorption of organic molecules to increase the efficiency of photocatalytic degradation. The organic pollutants, which are adsorbed on the meso porous (support) materials, have an opportunity to be degraded due to the appearance of hydroxyl radical on the support surface (Sohrabnezhad *et al.,*2009; Li *et al.,*2008).

A number of different solid supports have been applied for the formation of heterogeneous catalysts. Of these, the synthetic and bio-polymers, solid metal, amorphous silica or alumina, and zeolite-based catalysts have received the most attention. Zeolites are especially promising in their application as heterogeneous catalysts or catalyst carriers due to their ordered structure and high porosity. This structure allows for ready incorporation and immobilization of the catalyst onto the surface of the zeolitic pores, and not only enhances the surface area available for catalyst integration but also creates a highly structured and confined cavity which can positively affect photocatalysis. They can also facilitate catalyst recovery and product purification.

2.9. Zeolite and its Properties

Zeolites are crystalline aluminosilicates with regular porous structures of molecular dimensions, high surface areas, shape selectivity, and strong adsorptivity, widely applied in catalysis, separation, adsorption, and ion-exchange.

They are any of large group of minerals consisting of hydrated aluminosilicates used as cation exchangers and molecular sieves. As a typical porous material, zeolites can be divided into natural and synthetic zeolites. Natural zeolites are cheaper and more abundant, but have smaller channels as compared with synthetic zeolites. As a natural mineral resource, natural zeolites are easy to obtain and cause negligible chemical pollutions during the production process, but meet some difficulties in purification. Zeolites seem attractive candidates due to their unique uniform pores, super adsorption capacity and special ion-excchange ability (Xu and Langford, 1997; Kim *et al.,* 2006; Anandan and Yoon, 2003). Moreover, their inorganic framework keeps them from photo-decay. There are several advantages that zeolites afford as support or host of semiconductor particle. For example, the pore sizes of the host support material control the resulting particle size of the supported semiconductor. Particle size is a crucial factor in the dynamics of electron/hole recombination process especially in semiconductor nonmaterial, and that the movement of electrons and holes is primarily governed by the well-known quantum confinement (Chen and Mao, 2007). Generally, a decrease in particle size could be expected to lead to higher efficiency in photocatalysis (Tanaka *et al.,* 1997). This was because the bulk charge recombination of photo generated electrons and holes, dominant in the well-crystallized large semiconductor particles, were reduced by decreasing particle size. Reduction in particle size could also lead to a larger surface area and increased available surface active sites. Mordenite is a high-silica zeolite, in which the Si, Al content of the framework and the cation content of the erionite cavities are moderately variable.

In recent years, interest has arisen in the employment of zeolites in photochemistry for several reasons (Corma and Garcia, 2004; Hashimoto, 2003). Full photochemical stability, large thermal and chemical inertness, ability of the zeolite framework to actively participate in electron transfer processes as an either electron acceptor or electron donor and transparency to UV/Vis radiations above 240 nm, allow a certain percent of the excitation light to get into the opaque solid powders

and reach the channels and cages. (Dutta and Severance, 2011).The possibility of altering the chemical composition of the framework and surface charges allows the introduction of active sites that make these molecular sieves photoactive. For instance, one can synthesise zeolites to make them have photocatalytic activity by incorporation of hetero atoms into the framework, such as Ti rather than Si or Al. The net negative charges on the aluminosilicate framework are balanced by counter ions like Na^+, K^+ or other alkali and alkaline earth metal ions. These counter ions introduced in the pores play a very important role in introducing photocatalytic properties and can be readily exchanged by noble or transitional metal ions, providing an opportunity for modifying the photocatalytic property of zeolites. For instance, semiconductor incorporated zeolites have gained great importance as potential photocatalysts (Corrent *et al.,* 2001). Such assembly of multi-component host guest systems mainly constitutes antenna and relays of natural photosynthetic centres, including inorganic metal oxide clusters and organic electron-transfer photo sensitisers, since the guest becomes significantly stabilized by incorporation.

Zeolites have high adsorptive ability for organic compounds in solution, which can concentrate reagents in the proximity of the photo sensitizer. This strong adsorptivity contributes to the success of the photocatalytic reactions (Starosud *et al.,*1999). In some cases, the photo sensitizer absorbs light and reaches an excited state, and this state offers the potential to transfer energy to substrates; hence, the substrates become electronically excited even if the substrates have not directly absorbed light. The three coordinated aluminium sites on the framework and non-framework aluminium sites are normally considered to be Lewis acid sites. Additionally, charge compensating cations present in the pores of zeolite act as Lewis acids, and the framework oxygen represents a base. In particular, the oxygen atoms adjacent to Al (Si–O–Al oxygen) are more basic because of a larger negative charge on the oxygen. The Lewis acidity is connected to the electron-accepting property and Lewis basicity to the electron donating property (Hashimoto , 2003). The latter factor can lead to dramatic changes and modifications in the electronic states and conformational mobility of guests within zeolites (Marquez *et al.,* 2002). All these unique characteristics make zeolite-based materials attractive to scientists in the field of photocatalysis.

2.10. Methylene Blue (MB) Dye as Pollutants

The common target pollutants include aromatic compounds such as phenol, toluene, and chloro-benzene as well as dyes such as Rhodamine B, Acid Red 114, ethyl violet, and methylene blue. The dyes are of great interest as they are usually hard to degrade by conventional methods. Their remaining concentrations can also be easily determined by measuring the light absorbance of the reaction suspension or filtered sample. Methylene blue (MB) is a heterocyclic aromatic chemical compound (Figure 1) with molecular formula $C_{16}H_{18}N_3SCl$. It has number of applications in various fields. It is used as a dye for a number of staining procedures such as Wright's stain, Jenner's stain etc. Since it is a temporary staining technique, MB is also used to examine RNA or DNA under the microscope or in a gel. It is also used as an indicator to determine if a cell such as yeast is alive or dead. Beside these numerous applications, MB has lot of adverse reactions in environment and on human being such as hypertension, mental confusion, staining of skin, nausea, discoloration of urine, anaemia, precardial pain, headache, vomiting, bladder irritation, fever and abdominal pain. Dye pollutants from industries are important source of MB contamination. Large amount of unconsumed MB produced by chemical industries are discharged into the water every day. Presence of this dye in water causes considerable damage to the aquatic environment and human being coming in its contact. It is necessary to remove this compound from water. Several methods are used for this purpose including chemical precipitation and biological oxidation. Photocatalysis is one of the promising and effective method used for degradation of organic compound and dyes (Pawar and Lee, 2013; Lavand and Malghe, 2015). Mthylene blue is chosen as model pollutant of dye in this study. At room temperature it appears as a solid and is odorless and a dark green powder, which yields a blue solution when dissolved in water. The absorption maxima of MB (λ_{max} = 664 nm) was used for the analysis during degradation MB dye.

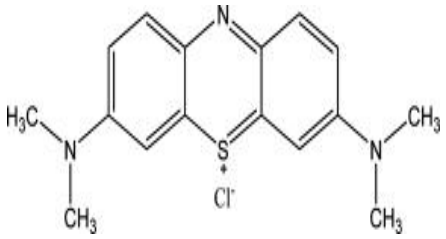

Figure 1.Structural formula of methylene blue

Photocatalysis mechanism (Hoffman *et al*., 1989):

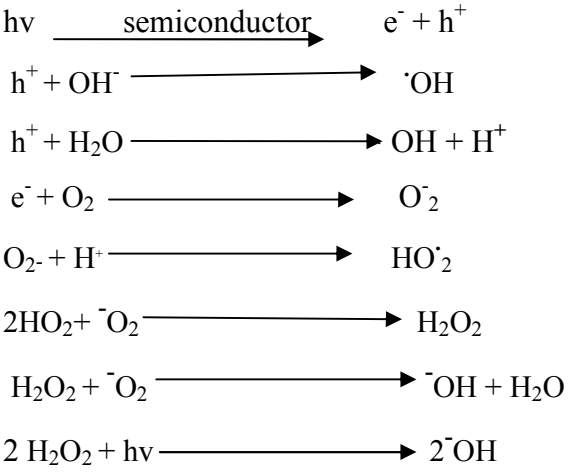

The radicals can attack the C–S^+=C functional group in MB, which is in direct Coulombic interaction with the surface of photocatalyst. Therefore, the initial step of MB degradation can be ascribed to the cleavage of the bonds of the C–S^+=C functional group in MB. The passage from C–S^+=C to C–S (=O)–C requires the conservation of the double bond conjugation, which induces the opening of the central aromatic ring containing both hetero atoms, S and N. The origin of H atoms necessary to C–H and N–H bond formation can be proposed from the proton reduction by photo-generated electron/hole (Houas *et al.,* 2011). The hydroxyl radical existing on the surface of photocatalyst accelerated the degradation of MB.

2.11. The Synthesis methods of Nanocomposite

There are several synthetic routes to synthesize nanosized materials. Some of the techniques are given below.

2.11.1. Precipitation Method

The principle of this method is based on the formation of aqueous solutions of the precursor followed by thermal decomposition until oxide formation.The strategy involves the simultaneous occurrence of nucleation, growth, and agglomeration processes.This sub process that participates in the whole reaction is modulated by a stabilizing agent. ZnO NPs with average crystallite size, 20nm, have been produced by the application of this strategy.In typical procedure; poly ethylene

glycol solution will be syringed in to three neck flask.Then znicacetate dehydrate and ammonium carbonate aqueous solution is dropped into the flask at the same time with vigorous stirring.After reacting for 2 h at room temperature , the precipitates is washed and filtered with ammonia solution (pH = 9) and anhydrous ethanol for several times ,and dried under vacuum for 12 h. Finally, the precursors are calcined at 450^0 C for 3 h and milled to obtain ZnO Nano-particles (Hong *et al*., 2009).

2.11.2. Incipient Wetness Impregnation Method

Incipient wetness impregnation method is commonly used method for synthesis of heterogeneou s catalysts.Typically; the active metal precursors are dissolved in aqueous or organic solution. Then the metal containing solution is added to a catalyst support the same pore volume as the volume of solution that added. The catalyst can be dried and calcined to drive off the volatile components within the solution, depositing the metal on the catalyst surface.

2.11.3. Sol-gel Method

The sol-gel process also known as chemical solution deposition is a wet chemical technique widely used in the fields of materials science and ceramic engineering. Such methods are used primarily for the fabrication of materials (metal oxide) starting from chemical solution that acts as the precursor for an integrated network of either discrete particles or network polymers. Typical precursors are metal alkoxides which undergo various forms of hydrolysis and poly-condensation reactions. Using inorganic salt or metallic alcohol salt as precursor nano powder can be obtained through gelation process by hydrolytic poly-condensation and some post treatment process. Specifically zinc acetate dihydrate ($Zn(CH_3COO)_2.2H_2O$), 2methoxyethanol ($CH_2(OCH_3)CH_2OH$) and monoethanolamine ($CH_3CHOHNH_2$) are used as precursor, solvent and stabilizer, respectively (Jang *et al*., 2010).

2.11.4. Hydrothermal Method

Nano-particles can also be synthesized by this technique which is also known as solvo-thermal technique (Wang *et al.,* 2009). The reactions are carried out in an autoclave at a pressure of 2000 pounds per square inch and a temperature of 200˚C or higher. Nanoparticles prepared by this method show better crystallinity and grain size. Nano photocatalyst with specific sizes and

morphology can be synthesized by continuous hydrothermal technique (Teja *et al.,* 2002). Reaction kinetics can be increased by microwave heating during hydrothermal technique (Komarneni *et al.,* 2002). Microwave hydrothermal technique needs lower temperature as 150^{o}C and shorter time as 25 min as compare to conventional hydrothermal technique. It is also a single step, fast and easy technique for the preparation of nano photocatalysts.

2.12. Characterization of Photocatalysts

2.12.1. X-Ray Diffraction

There are different techniques to characterize the crystalline materials. The basic techniques are X-ray diffraction is non-destructive analytical technique that can be applied for the identification of unknown specimens and for the determination of materials properties. It is the most important and beneficial technique in solid state chemistry and it has been applied for the fingerprint characterization of crystals and for the determination of their structures. This method requires an X-ray source (monochromatic or of variable λ), the sample (single crystal, powder or solid piece) which is under investigation and a detector (radiation counter or photographic film) that takes the diffracted X-rays.

2.12.2. UV-Vis Analysis

The optical absorption spectra and band gap of the as-synthesized photocatalyst was determined using UV/Vis spectroscopy at Haramaya University research laboratory. Then the absorbance of the photocatalyst solution was measured using a quartz tube, scanning over 200-800 nm.

2.12.3. AAS Measurement

As-synthesized ZnO,CdS/ZnO/Ag_3PO_4,and zeolite supported CdS/ZnO/Ag_3PO_4 nanocomposite was analsized using AAS instrument and the percent of Zn ,Cd and Ag metals in as-synthesized photocatalyst sample was calculated using the following formula.

$$\text{Percent of Metal (M \%)} = \frac{sample\ conc.(ppm)\ \ x\ \ volume\ \ of\ \ diluted\ \ to}{mass\ of\ \ sample\ \ taken\ \ x\ \ 1000} X\ \ 100$$

2.12.4. Scanning Electron Microscopy

SEM is a type of electron microscope which provides the information about sample's surface topography,composition and other surface properties suchas electricalconductivity.In scanning electronmicroscopy (SEM), it is possible to observeandcharacterize the heterogeneous organic and inorganic materials on a nanometer (nm) to micrometer (μm) scale. A three-dimensional-like image of the surfaces of a very wide range of materials can be taken. The basic constituents of the SEM are the lens system, electron gun, and electron collector, visual and photo-recording cathode ray tubes (CRTs) and associated electronics. In scanning electron microscope technique, the electrons from a focused beam are rastered across the surface of the material. Then, electrons reflected by the surface of the sample and emitted secondary electrons are detected in order to give the surface topography of samples like catalysts, polymers and crystals. It is a common method for examining the particle size, magnetic domains, crystal morphology, and surface defects.

2.12.5. Fourier Transforms Infrared Spectroscopy (FTIR)

Fourier transform infrared spectroscopy (FTIR) is a technique which is used to obtain an infrared spectrum of absorption or emission of solid, liquid or gas. An FTIR spectrometer simultaneously collects high spectral resolution data over a wide spectral range. It is ideal for the identification of functional groups present within a sample. Fourier Transform Infrared Spectroscopy (FTIR) was used to characterize the presence of specific functional groups such as C=O, -NO_2, C-N, and C-F; just to name a few, are all associated with characteristic infrared absorptions in the materials. The presence of different functional groups in as-synthesized nano materials was characterized by Fourier Transform Infrared Spectroscopy (TFIR).

2.12.6. Photoluminescence (PL)

Spectroscopic and electroanalytical techniques are used to evaluate the efficiency of charge separation and characterization of the heterostructure. Photoluminescence (PL) spectra helped us to trace the fates of the photogenerated electron/hole pairs. For effective photocatalytic reaction the photogenerated electron/hole pair should follow the first path, thus, should not recombine. PL

spectroscopy concerns monitoring the light emitted from atoms or molecules after they have absorbed photons (Skoog and Leary, 1992: Gfroerer, 2000). It is suitable for materials that exhibit photoluminescence. PL spectroscopy is suitable for the characterization of both organic and inorganic materials of virtually any size, and the samples can be in solid, liquid, or gaseous forms. The sample's PL emission properties are characterized by four parameters: intensity, emission wavelength, bandwidth of the emission peak, and the emission stability (Qu and Peng, 2002). The emission intensity of the as-synthesized nanocomposites was characterized by PL.

3. MATERIALS AND METHODS

3.1. Experimental Sites

Preparation of nanocomposites, photocatalytic degradation and AAS experiment were conducted at Haramaya University Chemistry Research Laboratory; FTIR was done at Addis Ababa University; XRD, SEM-EDX, UV-Vis analysis were determined at the Institute of Catalysis and Petroleum Chemistry, in Madrid, Spain.

3.2. Apparatuses and Instruments

Powder X-ray diffraction pattern was recorded with X´Pert Pro PANalytical with CuKα radiation (λ=1.5405Å). The data were registered with 2θ steps of 0.02º and accumulation times of 20s. The elemental composition of the nanocomposite was determined using AAS (BUCK) instrument (Model-210VGP, Method Air/acetylene, Current 1.5 mA, Slit 0.7 nm), Pulse =Wide,Wavelength at 376.5 nm). Band gap of the as-synthesized materials and photo degradation of the model pollutant dye was monitored using UV–VIS (SANYO, SP65 spectrophotometer). Other apparatuses like pH meter (MP 220), analytical balance (OHAUS, made in Switzerland), Oven (Contherm 260M), furnace (BiBBY, Stuart), Magnetic stirrer, Mortar and pestle, crucible, thermometer, beakers of different sizes.

3.3. Chemicals and Reagents

All chemicals are analytical grade and are bought from (SigmaAldrich). Zinc nitrate hexahydrate $Zn(NO_3)_2.6H_2O$,Cadmium sulphate hydrated ($CdSO_4.8H_2O$), Sodium sulphide (Na_2S), $AgNO_3$ and Na_2HPO_4,were used as the precursors of ZnO, CdS,and Ag_3PO_4, respectively. Commercially available synthetic zeolite (Mordenite) was used for supporting the as-synthesized ternary nanocomposite. Methylene Blue was used as a model of organic contaminant for investigating photocatalytic activities of the as-synthesized photocatalysts.

3.4. Synthsis of Nano-composite

3.4.1. Synthesis of ZnO Nanoparticles

ZnO nanoparticle was synthesized by precipitation method. 0.1M of Zinc nitrate hexahydrate ($Zn(NO_3)_2.6H_2O$) and 0.1M (10.6g) of sodium carbonate (Na_2CO_3) solution was separately prepared by dissolving required mount of $Zn(NO_3)_2.6H_2O$ and Na_2CO_3 in 100 mL of deionized water.The $Zn(NO_3)_2H_2O$ solution was slowly added into Na_2CO_3 solution and the mixture was stirred continuously for 3 h. The precipitate resulting from the reaction between the two solutions was allowed to settle down for 24 h, filtered with 0.2 μm membrane filter (Whatman) and was washed three times each with DI water and ethanol. The precipitate was dried at 100^oC to form the precursor for ZnO. The precursor obtained, after drying, was calcined at 300^oC for 12 h in programmable furnace to get the nano ZnO particles (Chen *et al.,* 2008).The product was labeled as ZnO (S1).

3.4.2. Synthesis of Ag_3PO_4 Nanoparticles

Ag_3PO_4 was prepared by chemical precipitation method in the dark using silver nitrate ($AgNO_3$) and disodium hydrogen phosphate (Na_2HPO_4) as raw materials. The $AgNO_3$ solution (0.1M) was prepared by dissolving 19.987g of $AgNO_3$ powder in 150 mL deionized water in dark condition. Similarly 0.1M Na_2HPO_4 solution (solution was prepared by dissolving14.2g of Na_2HPO_4 powder in 100 mL deionized water. Then after, $AgNO_3$ solution was added drop by drop into Na_2HPO_4 solution with continuous stirring for 3h in dark room and the precipitation so generated was made to settle down for 12 h. The resulting precipitate was filtered from the mother liquor and washed with double deionized water four times followed by ethanol two times. It was then, dried at 60^oC for 12 h and finally calcined at 300^oC for 2 h to get Ag_3PO_4 nano-composites labled as (S2) (Bi *et al.,* 2011).

3.4.3. Synthesis of CdS Nanoparticles

Cadmium sulphate hydrate ($CdSO_4 \cdot 8H_2O$) (20.84 g) and equal molar amount (24 g) of sodium sulfide (Na_2S) was dissolved in 100 mL of deionized water separately. The two separated solution were mixed through magnetic stirrer and the obtained precipitate filtered and washed several times by deionized water and ethanol to remove impurity. The obtained precursor was

dried at 300^{o}C for 2 h in hot air oven to get nanosized CdS particle. The product was labeled as CdS (S3) nanoparticles (Bi *et al.,* 2011).

3.4. 4. Synthesis of Ag_3PO_4 /ZnO Nano-composite

For the preparation of Ag_3PO_4/ZnO heterojunction structure, 0.1M (28.85 g) of Zn $(NO_3)_2.6H_2O$ and 0.1M (10.282 g) of Na_2CO_3 were separately dissolved in 100 mL deionized water and the two solutions were mixed together in the beaker. Second, 0.1M (19.98 g) of $AgNO_3$ and 0.1M (0 .42 g) of Na_2HPO_4 were dissolved separately in to 150 mL and 100 mL distilled water respectively and these solutions were mixed together as well. Then the second solution (mixture) was added into the first and the combined mixture stirred continuously for 3 h. The precipitate so formed from the reaction between the two solutions was allowed to settle down for 24 h, then filtered and washed three times each with DI water and ethanol. The final precipitate was dried at 100^{o} C for 5 h and calcined at 350^{o} C for 3 h in a programmable furnace to get nanocomposite Ag_3PO_4/ZnO (Chen *et al.,* 2008). The product was labeled as Ag_3PO_4/ZnO (B1).

3.4.5. Synthesis of CdS/ZnO Nano-composite

Zinc nitrate hexahydrate 0.1M (23.85 g) of $Zn(NO_3)_2.6H_2O$ and equal molar amount (8.16 g) of sodium carbonate (Na_2CO_3**)** solution was prepared separately by dissolving 100 mL deionized w ater.$Zn(NO_3)_2.6H_2O$ solution was added into sodium carbonate (Na_2CO_3**)** solution and the mixture was stirred magnetically until a homogeneous white solution was obtained. Then, (0.1M) 4.168 g deionized water matrix of cadmium sulphate octahydrate ($CdSO_4 \cdot 8H_2O$) solution was added to the above solution. After 10 min, (0.1M) 4.80 g of sodium sulfide solution (prepared in deionized matrix) was added to the above colloidal solution drop by drop with continuous stirring. The precipitate so formed from the reaction between the two solutions was allowed to settle down for 24 h, then filtered and washed three times each with DI water and ethanol. Washing with the same as for the uncoupled particles, and the product was then dried in a hot air oven at 100^{o}C for 12 h.Then calcined at 300^{o} C for 2 h in furnace to get CdS/ZnO nanocomposite labled as (B2) (Jana *et al.,* 2014).

3.4. 6. Synthesis of CdS/ZnO/Ag_3PO_4 Nano-composites

The ternary nano-composite was synthesized according to the procedure developed by (Dong, *et al*., 2006). The nanosized CdS/ZnO/Ag_3PO_4 was prepared by precipitation method using, solutions of cadmium sulphate octahydrate ($CdSO_4 \cdot 8H_2O$), sodium sulfide, zinc nitrate hexahydrate ($Zn(NO_3)_2.6H_2O$), $AgNO_3$ and Na_2HPO_4 as precursors. For this purpose, 0.1M of the respective salts of the precursors were separately dissolved in DI water and then mixed together to get a precipitate. Upon the filtration the precipitate was separated out, washed three times with DI water and ethanol filtered again and then dried in an oven for 12 h at 100^o C. The final product was calcined for 1h at 300^o C, this was prepared at four different ratios of the precursors (Table 3).

Table 1.Designation of the as-synthesized photocatalyst

Sample code	Experimental composition
S1	100% Zn
S2	100% Ag
S3	100% Cd
B1	10% Ag, 90% Zn
B2	10% Cd, 90 % Zn
T1	15% Cd, 80% Zn and 5% Ag
T2	10%Cd, 80% Zn and 10% Ag
T3	20% Cd, 70% Zn and 10% Ag
T4	25%Cd, 70% Zn and 5% Ag

3.4.7. Synthesis of Zeolite Supported CdS/ZnO/Ag_3PO_4 Photocatalyst

The zeolite supported ternary nano-composite material was prepared by impregnation method. The metal precursors were separately dissolved in DI water. Then the metal containing solution was added into photocatalyst support solution. Then the mixture of the two solutions (the metal precursors and commercial zeolite (Mordenite, SiO_2/Al_2O_3 ratio of 20) was stirred for 12 h. The precipitate formed from the reaction between the two solutions was allowed to settle down for 24 h, then filtered and washed three times each with DI water and ethanol. Then product was dried in an oven for 24 h at 100^o C. After solvent evaporation, the solid was dried and crushed by in mortar and pestle.The powdered mixture was then calcined to drive off the volatile component at 300^{o}C for 1h to get the zeolite supported nanocomposite. Two different ratio of zeolite supported nano-composite were prepared by using the same procedure.

3.5. Characterization of As-Synthesized Photocatalysts

The as-synthesized photocatalysts were characterized using AAS, UV-Vis, FTIR, XRD, PL, SEM and EDS.

AAS Measurement

The metal compositions of the as-synthesized CdS/ZnO/Ag_3PO_4 nanocomposite was analyzed using AAS instrument at Haramaya University and the percent of Cd, Zn and Ag metals in as-synthesized photocatalyst samples was calculated using the relation:

$$\text{Percentage (\%) of Metal} = \frac{sample\ conc.(ppm)\ \ x\ \ volume\ \ of\ \ diluted\ \ to}{mass\ of\ \ sample\ \ taken\ \ x\ \ 1000} X\ \ 100$$

UV-Vis Analysis

The band gap energies of the as-synthesized photocatalysts were determined using UV/Vis spectroscopy at Addis Ababa University. The absorbance of the photocatalyst in the solid state was measured using a plate by scanning over 200-800 nm.

The FTIR Study

The FTIR spectrum of powder nanocomposite was measured at Addis Ababa University in the frequency range (400-4000 cm^{-1}).

XRD Study

X-ray diffraction is non-destructive analytical technique that can be applied for the identification of unknown specimens and for the determination of materials properties. It is the most important and beneficial technique in solid state chemistry and it has been applied for the fingerprint characterization of crystals and for the determination of their structures.XRD (X'Pert Pro PANalytical equipped with an X-ray source of a CuKa radiation(wavelength of 0.15406 nm) pattern was determined for all of the as-synthesized powders) instrumental techniques.

Photoluminescence (PL) Study

Photoluminescence (PL) spectra were done at Addis Ababa University using a Fluorolog photoluminescence spectrometer (Horiba Jobin Yvon,Japan). The spectra were obtained in the range of 360–560 nm using 325nm laser excitation.

3.6. Photocatalytic Degradation Studies of Methylene Blue (MB)

Photo catalytic degradation of MB was carried out in duplicate at ambient temperature. For the purpose, required amounts of the as-synthesized photocatalyst powder and 100 mL of aqueous solution of MB were taken in a reactor tube. The resulting suspension was constantly stirred for 30 min in the dark before irradiation to reach at adsorption equilibrium. During the irradiation, the photo-reactor was kept under magnetic stirring for achieving a homogeneous suspension to promote the adsorption of dye on the surface of photocatalyst (Xu *et al.*, 2011). A 10 mL portion of each sample suspension was drawn at 30 minutes interval. The suspension was centrifuged at 3000 rpm for 15 min and filtered to remove the catalyst particles before measuring its absorbance using quartzes cells (10 mm optical path length). Decolorization was observed in terms of change in intensity of the MB dye at its λ_{max}(664 nm). The percentage photo catalytic degradation of dye was calculated from the following equation (Hong *et al.*, 1999):

$$\text{Percent Degradation} = \frac{A_o - A_t}{A_o} \times 100$$

Where A_0 is absorbance of dye at initial stage, A_t is absorbance of dye at time "t".

3.7. Effect of Operating Parameters

Various operating parameters affect the rate of photo catalytic degradation of organic pollutants or dyes in west waters. The operating parameters investigated in this work were pH, calcination temperature, catalyst loading, zeolite loading, and initial dye concentration. These parameters were studied one after the other as they influence the photo catalytic activity of as-synthsized nanocomposite in degradation of dyes.

Effect of Solution pH

The effect of pH on the rate of photo catalytic degradation of MB was investigated in the pH range of 2 to12. The pH was maintained each time by using 1M HCl or 1M of NaOH and measured using a pH meter (MettttlerToledo MP220).

Effect of initial concentration of dye (MB)

Dye concentration is very important parameter in wastewater treatment.Hence the effect of dyes on the rates of photocatalytic degradation was studied by taking different concentrations of MB solution and fixed amount of as-synthesized photocatalyst keeping other factors constant.

Effect of photocatalyst loading

To avoid excess use of photocatalyst within the system and to ensure total absorption of efficient photons, the optimum mass of the photocatalyst has to be found (Gerven *et al.,* 2007; Chiou *et al.,* 2008; Silva *et al.,* 2009).To this effect, the influence photocatalyst dose in degradation of MB dye was carried out by varying the catalyst dose from 0.01 to 0.4 g/L keeping other parameters constant.

Effect of calcinations temperature

The influence of calcinations temperature on photo catalytic degradation of methyleneblue (MB) was examined at various temperature ranges 300^{o}C, 400^{o}C, 500^{o}C and 600^{o}C and with constant catalyst loading, reaction time and MB solution.

Effect of irradiation time

For this study aqueous solution of MB in the presence of as synthesized nanocomposite irradiate with visible light at different time intervals keeping all other factor constant and the result were recorded.

Effect of Zeolite loading

The amount of zeolite employed as a support was evaluated by considering two different loads with a nanocomposite:zeolite ratio of 60:40 and 70:30. Commercial zeoliteY (zeolite, CBV21) was used as a support in this study.

Effect of light on the photo catalytic degradation

The effect of light on photo catalytic degradation of MB, experiments was examined both in the presence of light and catalyst and without light and photocatalyst with constant photocatalyst loading, initial dye concentration, irradiation time and pH. In each case during experiment, the photo reactor was kept maintained under magnetic stirring for 30 min achieving homogeneous suspension to promote the adsorption (Xu *et al.,* 2011).

3.8. Recyclability of the Catalyst

The catalyst's life time is an important parameter of the photo catalytic degradation process, so it is essential to evaluate the stability of the photocatalyst for practical application. In order to determine the stability of the synthesized photocatalyst during the photo catalytic reaction, the composite was taken to investigate the number of cycles the catalyst could possibly be used with no pronounced drop in its catalytic efficiency.The recycle test was performed four times in four consecutive trials; recovering the catalyst in between runs by centrifuging and decanting. For each new recycle, photocatalyst was reused for the degradation of afresh MB solution under similar condition after photocatalyst samples was recovered.

4. RESULTS AND DISCUSSION

4.1. Characterization of the As-Synthesized Powders

4.1.1. AAS Study

Atomic absorption spectroscopy was used for the determination of the elemental compositions of the sample. A 0.1 g of the as-synthesized T2 (10:80:10) powder was digested with conc. HNO_3,(8 mL) till clear solution appeared. The digested sample was filtered through whatman no.41 filter paper in 100 mL volumetric flask and the filtrate was brought to volume using deionized water. 1 mL of this solution was diluted further to 100 mL for AAS analysis. A series of working standard solutions of Zn, Ag and Cd were prepared from the stock solutions. Then, the metal percentages of as-synthesized photocatalyst were calculated using linear equations of the calibration curves which is indicated in the appendix (Figure 1- 3). The percentage of each metal in the composite was found to be almost similar with the measured theoretical composition (Table 2).

Table 2. Concentrations of Ag, Zn and Cd in ternary CdS/ZnO/Ag_3PO_4 nanocomposite

Element	Theoretical composition (%)	Actual composition (%)	Average absorbance from AAS read out
Cd	10	9.75	0.084
Zn	80	79.22	1.418
Ag	10	9.72	0.167

4.1.2. XRD Analysis

Figure 2 shows the XRD patterns of the as-prepared ZnO and the corresponding hybrids with Ag_3PO_4 and CdS. All the major diffraction peaks of ZnO (S1) nano-particles observed at 2θ values of 31.3^o, 33.5^o and 46.20^o are indexed to the hexagonally wurtzite structure. For Ag_3PO_4 (S2), the peaks identified at 2θ equal to 33.42^o, 52.86^o and 54.95^o represent body centered cubic structure. The most intense peaks observed at 2θ equal to 29.37^o, 44.7^o and 53.2^o indicate the formation of the more stable phase hexagonal wurtzite (greenockite) structure of CdS. The broadening of the diffraction peaks shows the formation of nanosized particles.

The diffraction peaks observed in Ag_3PO_4/ZnO (B1) nanocomposite showed diffraction peaks at 2θ values of 31.85°, 34.33°, 36.16° , 38.1°, 44.3°, 47.46° , 56.49° , 62.74°,62.7°, 64. °, 68.2° 77.4° and 81.5° represent hexagonal wurtzite structure of ZnO. No diffraction pattern attributable to Ag_3PO_4 was observed in this binary system possibly due to the small concentration (<5%) of the latter in the composite. In the case of CdS/ZnO (B2) binary system, most ofthe diffraction peaks observed could be ascribed to hexagonal wurtzite structure of the host crystal ZnO. However, diffraction peaks at 2θ values of 19.2°, 28.1° and 48.84° indicate the presence of hexagonal wurtzite (greenockite) structure of CdS in the binary system. The peaks of the CdS/ZnO binary system are found to be restrained compared to pure ZnO due to the amorphous nature of the CdS.

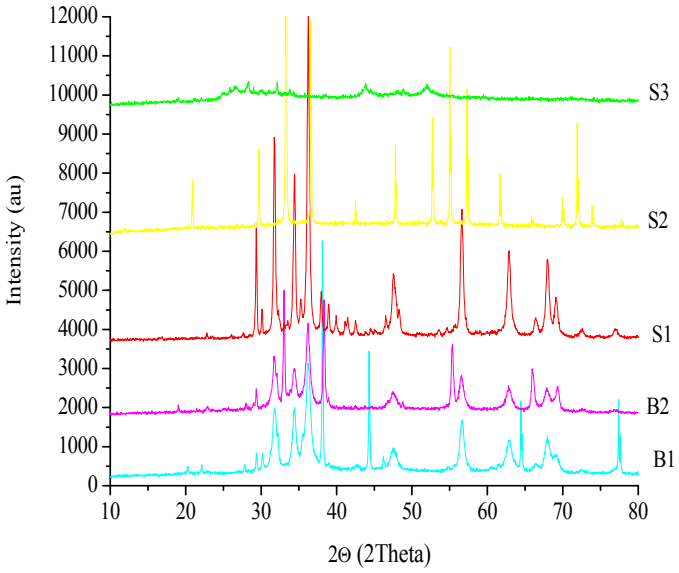

Figure 2. XRD patterns of S1, S2, S3, B1, and B2

Where, S1 = ZnO, S2 = Ag_3PO_4, B1 = Ag_3PO_4/ZnO, B2 = CdS/ZnO

For all the ternary systems, similar diffraction peaks were observed at 2θ values of 26.69°, 28.7 °, 31.7°, 34.37°, 36.27°, 43.95°, 47.5°, 52.3°, 56.5°, 62.99°, and 67.95°. Among these, diffraction peaks at 31.7°, 34.37°, 36.27°, 43.95°, 47.5°, 56.5°, 62.99°, and 67.95° could be attributed to hexagonal wurtzite structure of the host crystal ZnO; peaks at 2θ value of 31.7° and 36.27° could

be ascribed to body centered cubic structure of Ag_3PO_4 and peaks at 2θ value of 26.69°, 28.7 °, 43.95° , and 52.3° can be accounted for the hexagonal structure of CdS.

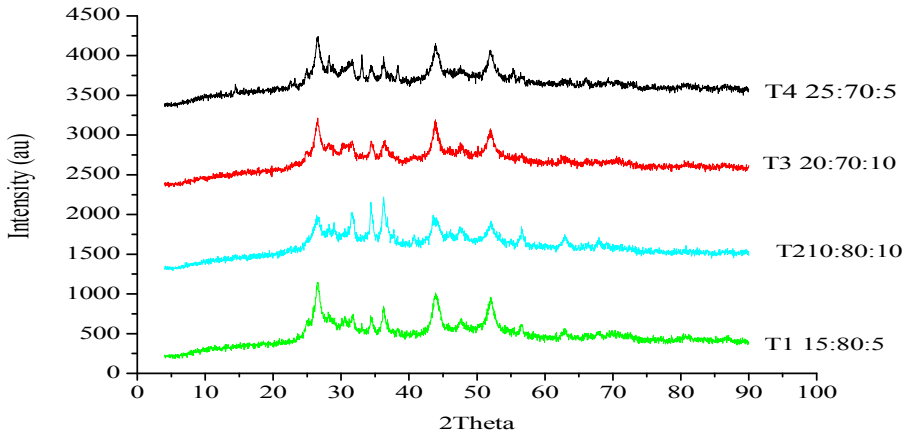

Figure 3. XRD patterns of T1, T2, T3 and T4

Where, T1 = $CdS/ZnO/Ag_3PO_4$ (15:80:5), respectively, T2 = $CdS/ZnO/Ag_3PO_4$ (10:80:10), respectively, T3 = $CdS/ZnO/Ag_3PO_4$ (10:70:20), respectively, T4 = $CdS/ZnO/Ag_3PO_4$ (5:70:25), respectively.

The ternary $CdS/ZnO/Ag_3PO_4$ nano-composite shows highest surface area (Table 3) compared with single and binary nano-composites. The difference in their surface area was due to the synergetic effect among the components such as ZnO, Ag_3PO_4 and CdS in the composite system (Li *et al*., 2008). The increase in the surface area was significant; hence, the larger surface area of $CdS/ZnO/Ag_3PO_4$ Nano-composite will benefit for the spatial separation of redox sites in the crystals which can enhance electron-transfer properties of the Nano-composite (Hermann *et al.,* 1986; Yang *et al.,* 2008). It is evidently observed that the size of the synthesized Nano-composite decreases in the ternary Nano-composite system because of heterogeneous nucleation effect (He *et al.,* 2010).

Average crystalline size of the synthesized nano-particles were calculated using Debye-Scherrer equation:

$$D = 0.89\lambda / \beta \text{ Cos } \theta \quad (4.1)$$

Where, β is the full width at half maximum (FWHM), θ is the angle between the incident and diffracted beams in degrees, λ is the X-ray wavelength in nanometers, D is crystallite size.

Table 3. Average crystallite sizes of the as-synthesized nanomaterials

Photocatalyst	2θ (degree)	β (radians)	D (nm)	Band gap (Eg) eV
S_1	36.16	0.0053	26.329	3.21
S_2	33.23	0.0023	59.354	2.43
S_3	28.19	0.0088	16.235	2.44
B_1	38.18	0.0038	38.610	2.26
B_2	36.27	0.0049	29.753	2.22
T_1	34.37	0.0030	48.346	2.13
T_2	31.74	0.0039	49.695	2.16
T_3	26.69	0.0053	26.886	2.16
T_4	26.71	0.0062	22.985	2.13
Tz 60:40	29.06	0.0043	31.236	2.07
Tz 70:30	26.14	0.0038	37.271	2.13

Based on the above approach, we estimated the average crystalline size of as-synthesized photocatalysts as shown in Table 3. Accordingly, all the as-synthesized materials were found to be in the nano range. We synthesized ternary systems in four compositions labeled as T1, T2, T3 and T4. Among these ternary nanocomposites, T1 and T2 were selected for further experiments based on the band gap results estimated from the Uv-Vis and the preliminary photocatalytic performance. In this work, T2 was selected for the subsequent immobilization onto a zeolite support where as T1 was supported onto polyaniline support to evaluate antimicrobial effects of the same by other member of the research group in our laboratory.

For this experiment, T2 was mixed with zeolite in two ratios. In the first case the percent composition was 70% T2 and 30% zeolite labeled as Tz (70:30) where as in the second case the percent composition was 60% T2 and 40% zeolite labeled as Tz(60:40). The XRD results of T2 and the supported T2 onto the zeolite are depicted in figure 4. In general, the peaks observed in the supported nanocomposite systems are restrained compared to the unsupported congener. This observation is evidenced by the small average crystallite size of the supported system (Tz 60:40). exhibited on Table 3. Despite this, most of the peaks in the unsupported nanocomposite T2 are also observed in the supported system. In the case of the supported systems, additional peaks are observed at 2θ values of 9.81°, 13.43 °, 22.3 °, 25.1°, 25. ° 6, 26.46 °, 28.2 °, 29.12 °, 31.53 °, and 52.3° attributed to mordenite type of zeolite. In this work, we selected Tz (60:40) for the subsequent experiments due to with improved photo degradation efficiency in visible light irradiation, the lower band gap energy and highest surface area of the system prevents the fast electron–hole recombination (Ansari *et al*., 2013).

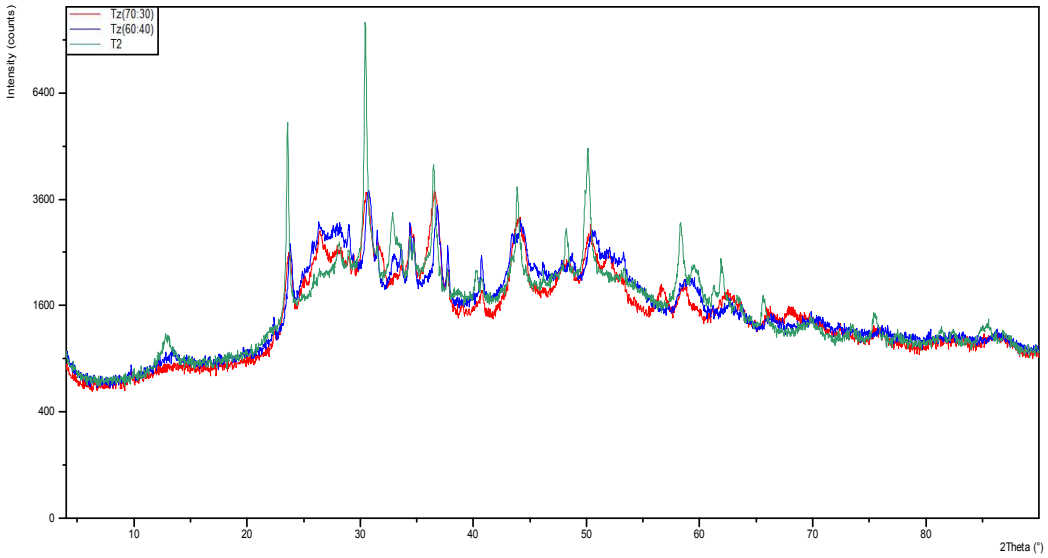

Figure 4. XRD patterns of T2, Tz (60:40) and Tz(70:30)

T2 is naked ternary nanocomposite and Tz (60:40) and Tz(70:30) are zeolite supported nanocomposites in the ratio as shown in the bracket.

4.1.3. UV-Vis Diffuses Absorption Spectra of As-synthesized Materials

UV–Vis diffuse absorption spectroscopic data of ZnO, Ag_3PO_4, Ag_3PO_4/ZnO, CdS/ZnO and CdS/ZnO/Ag_3PO_4 (T1, T2, T3, T4) and zeolite supported CdS/ZnO/Ag_3PO_4 (Tz) obtained from the plots of absorbance against wavelength is presented in Figure 5 . The intercept of the tangent line on descending part of the absorption peak at the wavelength axis gives the value of absorption maximum (λ_{nm}). Estimation of band gap energy using from UV-Vis absorption spectroscopy in dispersed samples some time may not provide clear tangential line when the peak is not well resolved for a given sample. This could probably happen when the scattering effect is as high as the optical absorption processes. In such case scattering screens the absorption peak, making the assignment of band gap energy (Eg) uncertain. To avoid this we use Tauc plot of absorbance against wavelength using equation shown below (Cao *et al*., 2012).

$$\alpha h\nu = A\,(h\nu - Eg)^{n/2} \qquad (4.2)$$

Where α, hν, A, and Eg are optical absorption coefficient, the photonic energy, proportionality constant, and band gap, respectively. The direct band gap of the prepared photocatalyst was determined from the plot of $(\alpha h\nu)^2$ vs hν was indicated in the (Figure 5) . Accordingly, the estimated band gaps estimated by extrapolating the straight line to the x-axis for ZnO, Ag_3PO_4, CdS, Ag_3PO_4/ZnO, CdS /ZnO and CdS/ZnO/Ag_3PO_4 (T1, T2, T3, T4, and Tz) were found to be 3.21, 2.43, 2.44, 2.26, 2.22, 2.13, 2.16, 2.16, 2.13 and 2.07 eV respectively.

Based on Kubelka-Munk equation (4.2) the band gaps for all the as-synthesized materials is displayed in Table 3. The calculated band gaps of the single systems Ag_3PO_4, CdS, and ZnO is found to be 2.43 eV, 2.44 eV and 3.21 eV. These findings are similar with previous reports made on these nanoparticles (Rawal *et al.,* 2012; Alebel, Nibret *et al.,* 2015; Pandey *et al.,* 2015). The binary systems Ag_3PO_4/ZnO (B1) and CdS/ZnO (B2) have exhibited calculated band gaps of 2.26 eV and 2.22 eV, respectively. The results obtained as such are in good agreement with the previously reported works (Liu *et al.,* 2013; Jana *et al.,* 2014).

In the ternary systems T_1, T_2, T_3 and T_4 the band gaps were recorded as 2.13 eV, 2.16 eV, 2.16 eV and 2.13 eV, respectively. As can be noted here, formation of ternary systems resulted in

further red-shift in the visible spectrum which result from the interfacial combination and matched band edges between the three semiconductors of synthesized nanocomposites ($CdS/ZnO/Ag_3PO_4$). Based on the band gap results of the ternary systems, we selected T2 for immobilizing the same to a zeolite support. The zeolite supported ternary system labled as Tz(60:40) was also run by Uv-vis to determine its band gap. The calculated band gap is found to be 2.07 eV. The zeolite support has appeared to shift the absorption band of ternary $CdS/ZnO/Ag_3PO_4$ (10:80:10) nanocomposite further to the visible region making it a better visible active nanocomposite photocatalyst.

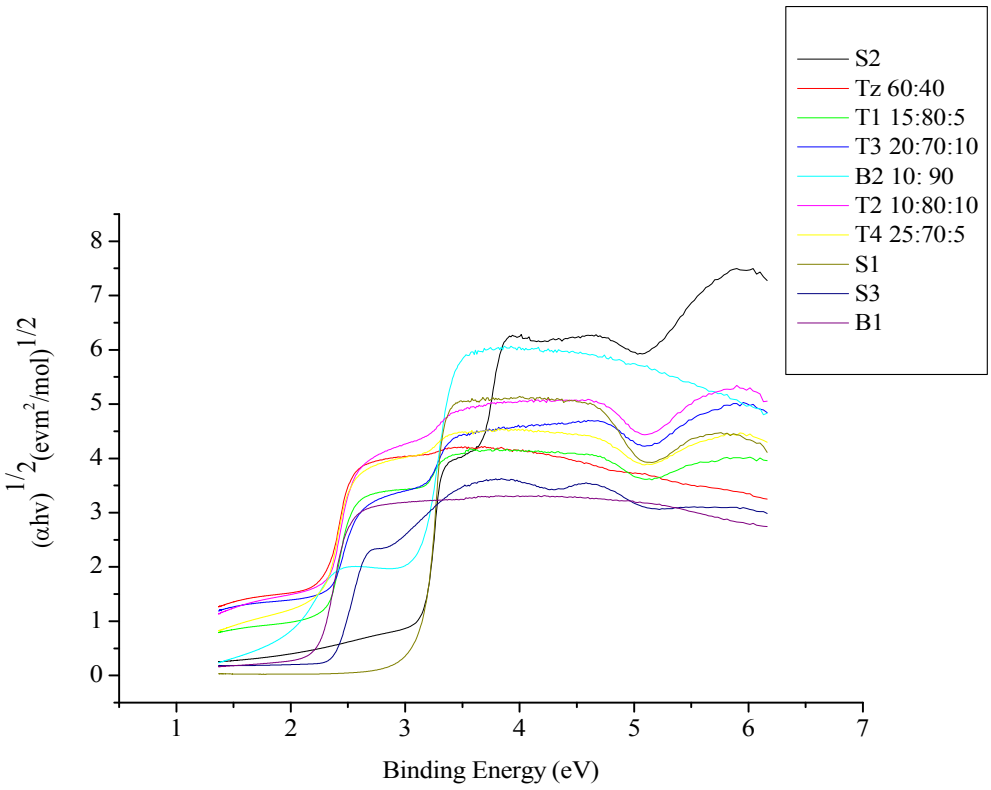

Figure 5. Uv-visible diffuse reflectance spectra of S1,S2,S3,B1,B2,T1,T2,T3,T4 and Tz 60:40

4.1.4. FourierTransform Infrared Spectroscopy Study of As-synthesized Photocatalyst

The selected surface functional groups of the naked and supported ternary nanocomposite (T2 and Tz 60:40) materials were analyzed by FTIR in the range from 400 to 4000 cm^{-1} (Figure 6).The FTIR spectrum of the synthesized nanocomposite material contains several bands with

remarkable features. Both samples (T2 and Tz 60:40) show bands at 3427cm^{-1} attributed to stretching modes of -OH group of water molecules adsorbed on the surface of photocatalyst (Wahab *et al.,*2013).The band located at around 457cm^{-1} is correlated to metal oxide bond (Zn-O), which confirms the formation of ZnO (Hong *et al.,* 2009). The band at 1370 cm^{-1} can be attributed to the C=O residue probably due to atmospheric CO_2 (Chira *et al.,* 2011). Band at 619.98 cm^{-1} can be ascribed to Cd–S stretching of synthesized nano-composite (Yang *et al.,* 2013).

Adsorption bands near 1015cm^{-1} are assigned to P-O^{-}group, which comprise the phosphate non-bridging oxygen portion of PO_4 tetrahedral in a chain structure (Shih, 2004; Ari and Spark,2001). The presence of weak band near 1604.07 cm^{-1} and 1500 cm^{-1} are assigned to H–O–H bending may due to the adsorption of moisture. All the bands between 400 and 750 cm^{-1} correlated to metal oxide bond (ZnO) (Kwon *et al.,* 2002; Silva and Zaniquelli, 2002; Kurien *et al.,* 2004). It is evident from the FTIR data that the Zn–O vibrational mode was more prominently observed, this clearly concludes the ZnO is host crystal and a strong coupling between ZnO with CdS and Ag_3PO_4 nano-composite materials (Shah *et al.,* 2013). Changes in FTIR spectra for zeolite supported nano-composites was shown in (Figure 6) band in region of 1620.87cm^{-1} and 1500 cm^{-1} was related to zeolite (Mohammad *et al.,* 2015). These imply certain chemical interactions between zeolite and as-synthesized nano-composite.

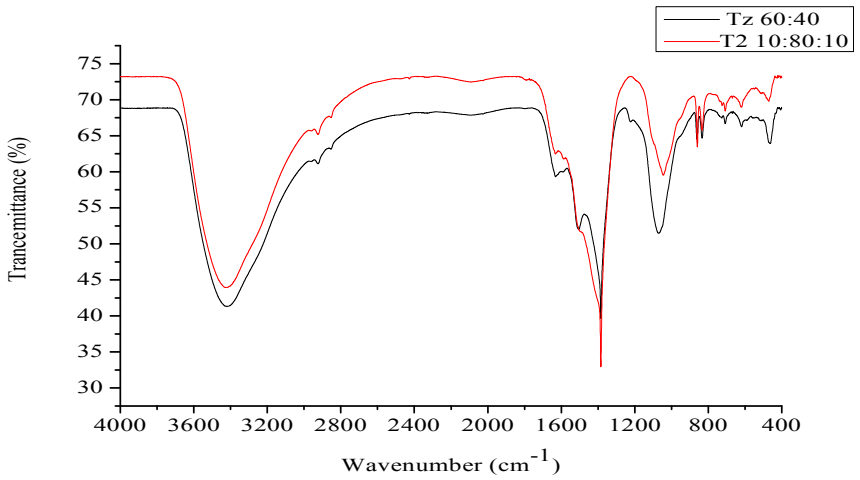

Figure 6. FTIR spectrum of synthesized nano-composite, a) T2 and b) Tz 60:40.

4.1.5. Photoluminescence (PL) Study of As-Synthesized Photocatalyst

The photoluminescences spectra of nanocomposite materials were shown in the Figure 7. It was observed that PL intensity of binary and ternary Nano-composite is much lower as compared to pure ZnO and their respective single nano-materials. Photoluminescence effect is present as the result of direct radiative recombination, lower recombination of generated carriers causes the decrease of light emission intensity. The order of intensity is ZnO (S1) > CdS (S3) > Ag_3PO_4 (S2) > CdS/ZnO (B2) > Ag_3PO_4/ZnO (B1) > T2 >Tz. It is in good agreement with the results obtained for photocatalytic degradation curves presented in the (Figure 11). In binary and ternary nano-composite system photo induced electrons and holes can be effectively separated and hence excitonic PL intensity goes down. This is because, lower the excitonic PL intensity, stronger the capacity of coupled materials to capture photo-induced electrons, higher the separation rate of photo induced electrons and holes, and higher the photocatalytic activity. It is evidently observed from Photoluminescence spectra that the zeolite supported ternary (Tz) nano-composite prepared in the present work showed relatively higher efficiency for photocatalytic degradation evidencing the dual role of zeolite (suppressing electron-hole recombination and increasing adsorption capacity) thereby enhancing the photo catalytic activity of synthesized nanocomposite system.

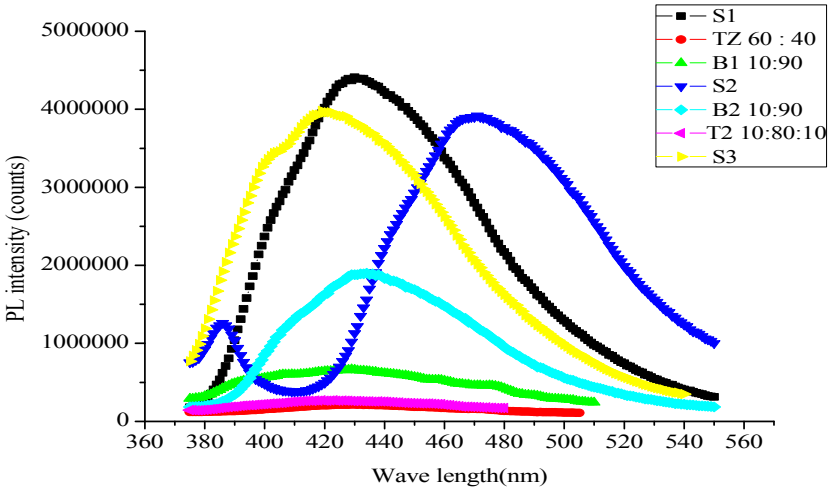

Figure 7. Photoluminescence spectra of synthesized nano-composite.

4.1.6. SEM Image Study of As-Synthesized Photocatalyst

The surface morphology of the naked T2 and zeolite supported Tz(60:40) nano-composites were investigated as shown in the(Figure 8 and 9). The SEM micrographs in both cases show irregular shaped particles with no distinct morphology. The EDX spectra show the presence of all the relevant components in both naked and zeolite supported ternary systems.

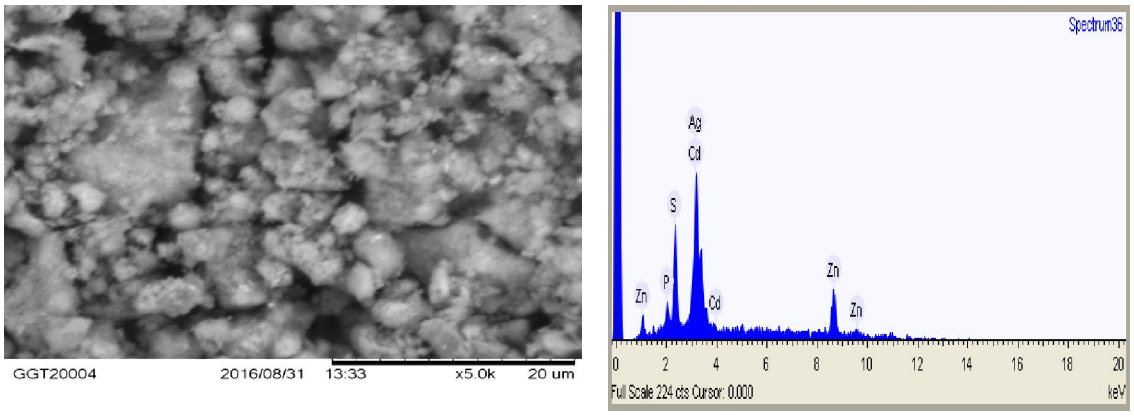

(a) (b)

Figure 8. Scanning electron microscopic image a) and EDX spectrum of T2

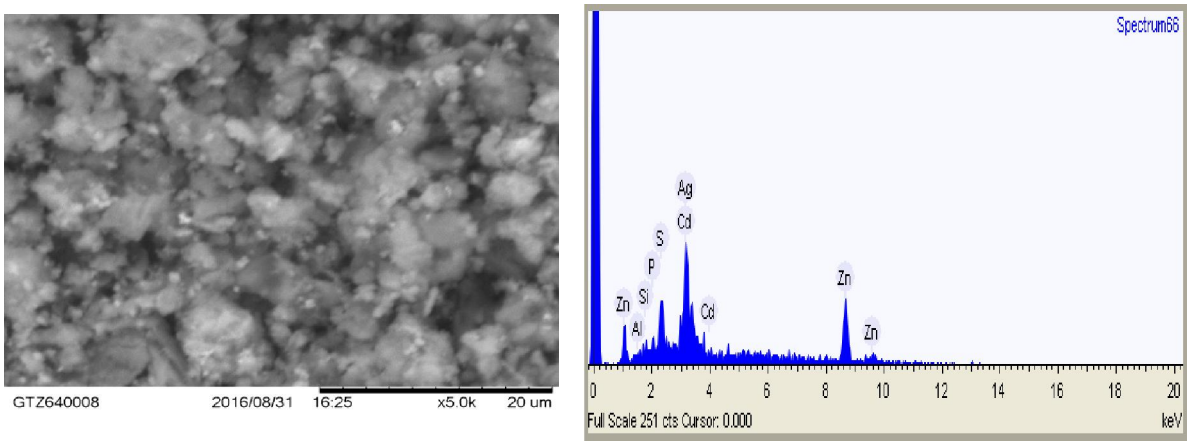

(a) (b)

Figure 9. Scanning electron microscopic image a) and EDX spectrum of Tz 60:40

4.2. Photocatalytic Studies

4.2.1. Comparison of Photocatalytic Activities of As-Synthesized Photocatalysts

It is known that the photo catalytic redox reaction mainly takes place on the surface of the photocatalysts and the improved surface properties significantly influence the efficiency of the photocatalysts (Yang *et al.,* 2008). In this work single, binary and ternary photocatalyst (ZnO, Ag_3PO_4, CdS, Ag_3PO_4/ZnO, CdS/ZnO and CdS/ZnO/Ag_3PO_4) materials were synthesized by precipitation method. The photo catalytic activities of synthesized nano materials were compared using water soluble model dye (MB) as reported (Saravanan *et al.,* 2013).The CdS/ZnO and Ag_3PO_4/ZnO composite systems show higher degradation of methylene blue under visible light irradiation than ZnO because of the retardation of back reaction between CdS and Ag_3PO_4 with ZnO which produces more number of charge carriers that would increase the degradation efficiency (Figure 10). Thus, the efficiency of photo generated electron–hole in CdS/ZnO and Ag_3PO_4/ZnO was higher than that of pure ZnO.

The highest percentage degradation of the photocatalysts for S1, S2, S3, B1, B2, T1, T2, T3, and T4 were 22.11, 45.02, 26.10, 29.78, 28.00, 61.87, 73.17, 43.31 and 36.21 respectively as indicated in the appendix (table 6).The results reveal that the lowest of all the photocatalysts in photocatalytic efficiency was pure ZnO (S1) nano-composite.This is due to the relatively higher electron-hole recombination and less efficient use of the visible irradiation for ZnO because of its wide band gap. The binary and ternary systems generally showed better catalytic efficiency compared to the single photocatalysts. This clearly indicates that the heterojunction or coupling created a condition that favors the enhancement of the degradation efficiency.

Also, the ternary photocatalyst (CdS/ZnO/Ag_3PO_4) exhibits the highest photocatalytic activity when compared with the binary photocatalysts (Ag_3PO_4/ZnO and CdS/ZnO). The reason for the enhancement of ternary nano-composite is that having more than one path for the formation of electron–hole pair because of the three different interfaces and the electron–hole pair recombination is prevented to the maximum extent in the ternary nanocomposite (Ansari *et al*., 2013; Vinod *et al.,* 2012). The nano-composite with percentage ratio of 10:80:10 (T2) systems showed highest photo catalytic activity when compared with other percentage ratio and hence selected for further study. Enhanced photo catalytic activity of T2 (10:80:10) is due to

effective loading of Ag_3PO_4 and CdS on ZnO nano-composite to create visible sensitive heterojunction which increases its photo absorption capacity in visible region.

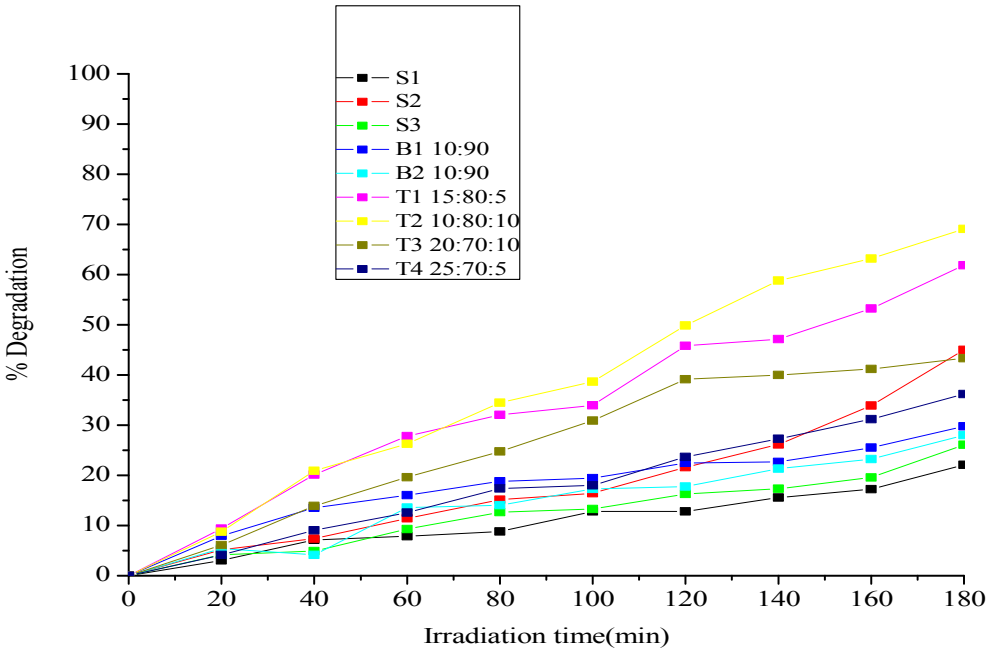

Figure 10. Comparison of photocatalytic activities of as-synthesized single, binary and ternary Photocatalysts

Where, S1 = (ZnO), S2 = (Ag_3PO_4), S3 = (CdS), B1 = (Ag_3PO_4/ ZnO), B2 = (CdS /ZnO), T1= CdS/ZnO/Ag_3PO_4 , (5:80:15), T2 = CdS/ZnO/Ag_3PO_4, (10: 80: 10), T3 = CdS/ZnO/Ag_3PO_4, (10: 70: 20), and T4 = CdS/ZnO/Ag_3PO_4, (5: 70: 25) respectively.

4.2.2. Comparison of photocatalytic activity of naked and zeolite supported nanocomposites

Nano crystals immobilized on supporting materials such as glass, sand, or zeolite can improve the separation efficiency (Anandan *et al.,* 2003). In an ideal case, the nano crystals would deposit as a monolayer covering the support surface to maximize the catalytically active surface area. In fact, the supported adsorbent such as zeolite on photocatalysts, can absorb pollutants and the pollutant, then, are exposed to the photocatalysts at high concentrations leading to materials removal process. This remarkable function due to the combination of zeolite and photocatalysts

can enhance the removal efficiency compared to the photocatalyst without supports.The effect of supports on the photocatalytic activity of as-synthesized ternary photocatalyst was studied using synthetic zeolite (mordenite) as a support for the photocatalysts.

Based on the results, the zeolite supported photocatalyst showed a higher activity than the photocatalysts without support as illustrated in (Figure 11). For the same irradiation time, the removal efficiency for target pollutants of unsupported and supported photocatalyst was 73.17%, 94.79% respectively. Our finding was similar to the result of other studies (Haileyesuse Tedla *et al*, 2015; Teketel Grima *et al.,* 2015). In their work, they carried out zeolite supported and unsupported ternary nano-composite used for photo catalytic degradation of MB and MO respectively and concluded that the zeolite supported was much more effective than unsupported ternary nano-composite.

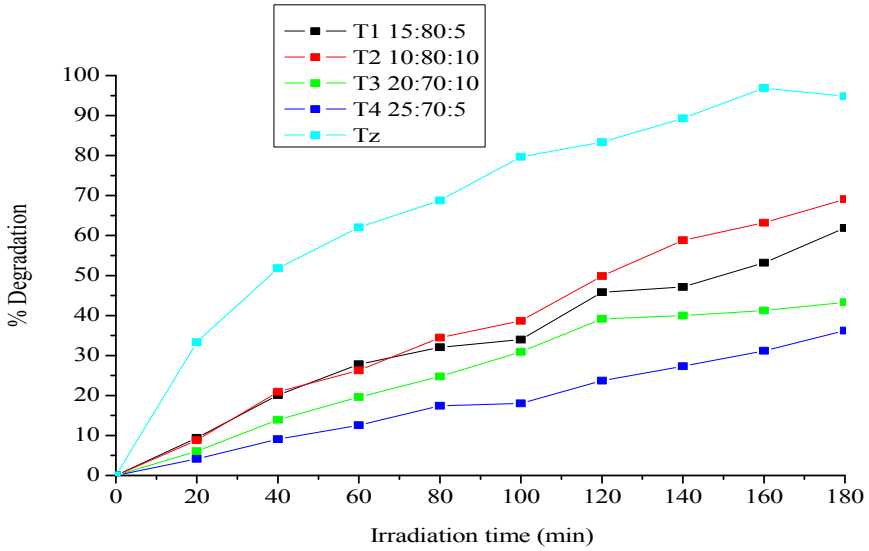

Figure 11. Comparison of the photocatalytic efficiency of zeolite supported and unsupported ternary Nano-composites as function of time

Where, T1 = CdS/ZnO/Ag_3PO_4, (5:80:15), T2 = CdS/ZnO/Ag_3PO_4 (10: 80:10) respectively, T3 = CdS/ZnO/Ag_3PO_4,(10:70:20), respectively and T4 = CdS/ZnO/Ag_3PO_4, (5:70:25) respectively.

This work demonstrates that the activity of the photocatalyst supported with zeolite was higher than that of synthesized bare photocatalyst (CdS/ZnO/Ag_3PO_4). This is due to the higher adsorption capacity, higher surface area, and fine dispersion of the photocatalyst in cavities of

the zeolite which are mainly responsible factors for the facilitation of higher photo catalytic activity. Fine dispersion of photocatalysts results in higher photo catalytically active sites on the zeolite surface (Sowbhagya and Sannaiah, 2014).

4.2. 3. Effect of Operating Parameters

4.2.3.1. Effect of pH

The pH can affect the catalyst-pollutant interactions and generation of redox species during irradiation (Tang *et al.,* 1997). Photocatalyst surface is predominantly negatively charged when the pH is increased beyond isoelectric point of photocatalyst. As the pH decreases, the functional groups are protonated, thus raising the positive charge of photocatalyst surface. The surface of photocatalyst will be charged negatively at higher pH and results in the increased adsorption of cationic molecules while in the reverse situation it would adsorb anionic molecules very easily (Rajabi *et al.,* 2013). In the meantime, the increased pH value increases the hydroxyl radical's generation (Chiang and Lin, 2013). But the degradation of organic molecules is repressed when the pH of solution is too high (pH > 12), because hydroxyl ions compete with organic molecules for the adsorption on the surface of the catalysts (Rajabi *et al.,* 2013). On the contrary, at low pH, the adsorption of cationic organic molecule on the photocatalyst surface is reduced, because the surface of photocatalyst is positively charged which results in the decrease in adsorption of cationic organic molecules. The effect of pH on the degradation of MB is also explained in similar way to the above. In addition, in the photocatalytic process, the number of photo generated electrons and holes that reach the surface of the particles determines the efficiency of the dye's degradation (Yao *et al.,* 2004).

To study the effect of pH on the degradation of MB, the experiments were carried out at various pH values, ranging from 2 to12 by adjusting with NaOH or HCl, the catalyst load 0.2 g/L and at 10 mg/L dye concentration (Figure 12). The percent degradation increased considerably with an increase in pH from 2 to 8 for as-synthesized nanocomposite and this indicates the percentage of decoloration is higher at basic condition than the acidic condition. Because MB is a cationic dye, its structure becomes positively charged when it is dissolved in water. As mentioned in literature

above the surface of the particles is negatively charged when the solution pH is higher than the zero point charge. These opposite charges between the solution and the surface of the particles enhance the degradation of MB. Therefore, we believed that the increase in the degradation rate at higher pH value can be explained as: a higher pH value could provide a higher concentration of hydroxyl ions that can react with the photo generated holes to form $OH^{\cdot}$ and subsequently enhance the degradation of MB. On other hand, the surface of MB is positively charged; the photo generated electrons can transfer to the surface of the particle and enter the molecular structure of MB which lead to the decomposition of MB(Qi *et al.,* 2008; Qi *et al.,*2009).In acidic or neutral pH medium the degradation rate of MB decreased because it can not provides enough hydroxyl groups to form $OH^{-\cdot}$. Besides, at lower pH, the photocatalyst would develop positive charge. As the dye is a cationic one, electrostatic repulsion would prevail which in turn is the reason for reduced interaction between the dye and the surface of the photocatalyst which lead to decreased photo catalytic efficiency. The photocatalyst exhibiting maximum rate of degradation (96.51%) at pH = 8 at 140 min. Unlike others, the percent degradation declined beyond this time. The general trend is, however, similar to previous studies done for photo catalytic degradation of MB dyes with Fe-doped ZnOand C-doped TiO_2 nano-particles (Rosari *et al.,* 2014; Xiao *et al.,* 2008).

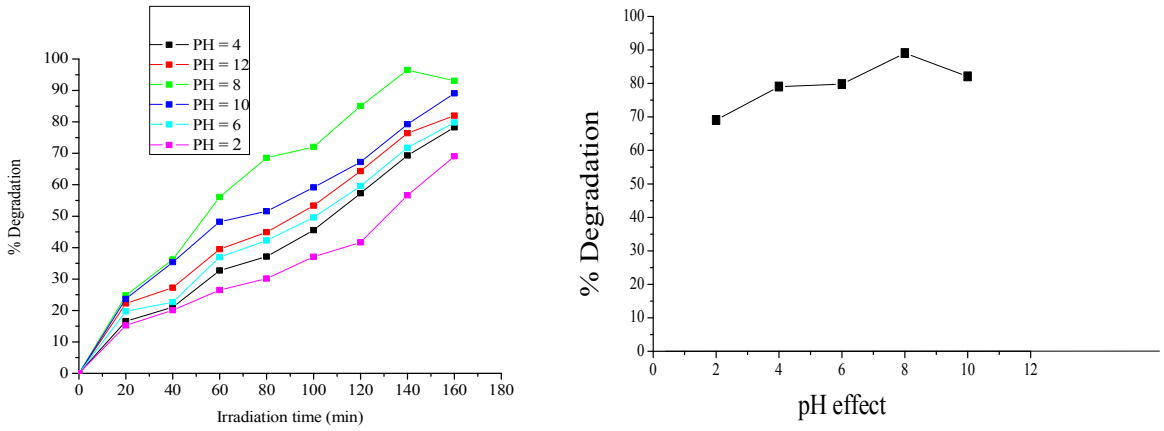

Figure 12. The effect of pH on the degradation of MB as function of irradiation time with catalyst loading 0.2 g/L & conc. of MB 10 mg/L , under visible light.

4.2.3.2. Effect of initial dye concentration

The photocatalytic degradation of dye was carried out by varying the initial concentration of dye from 10 to 30 mg/L in order to determine appropriate amount of dye dose. It was found that nano-composites exhibited a higher photo catalytic activity at a low dye concentration (10 mg/L) but showed decreased degradation efficiency at high initial dye concentration (Figure 13). This is because with increase in the dye concentration, the solution becomes more intense in color and the path length of the photons entering the solution is decreased resulting in only a few photons reaching the catalyst surface. Hence, the productions of hydroxyl radicals are reduced. Therefore, the degradation efficiency is reduced (Sowbhagya and Sannaiah, 2014). This negative effect is because of the following reasons: The number of dye molecules that are adsorbed on the surface of photocatalyst increase because of the increment in dye concentration. In addition, at a high dye (MB) concentration a significant amount of visible light is absorbed by the dye molecules (Alireza *et al.,* 2015). The generation of OH· radicals on the surface of catalyst is likely be reduced since active sites on the surface of the catalyst are occupied by the dye ions (Alireza *et al.,* 2015). Figure 13 Show that the maximum degradation of MB was achieved using 10 mg/L of dye concentration. The comparison of efficiency was done based on the percentage degradation at 20 min time interval under visible light.

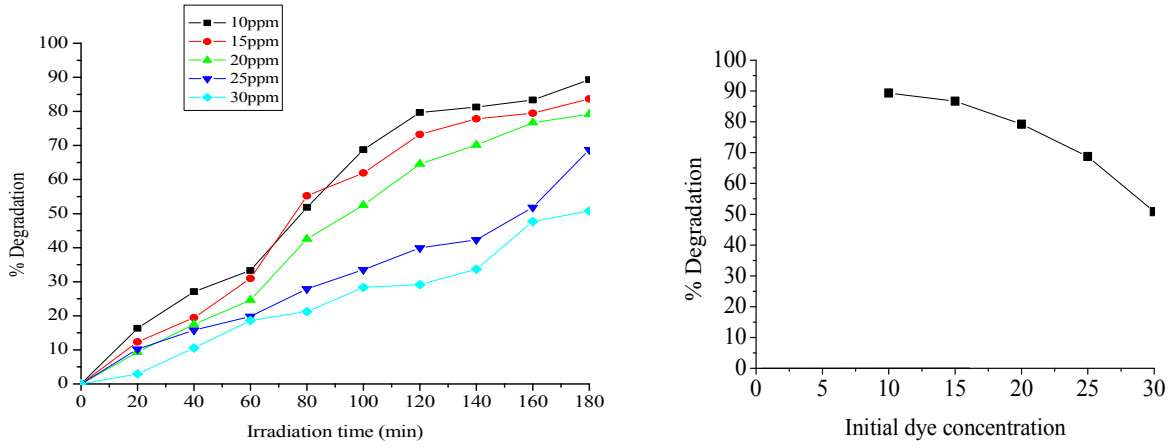

Figure 13. The Effect of initial dyes concentration on photocatalytic activities of as-synthesized nano-composite with respect to irradiation time.

4.2.3.3. Effect of photocatalyst loading

Influence photocatalyst dose in degradation organic pollutants was carried out by varying the catalyst dose from 0.01 to 0.4 g/L (Figure 14). In our study initially the degradation of MB increases with increasing in photocatalyst load from 0.01 g/L to 0.2 g/L and further increase of catalyst loading from 0.2 g/L to 0.4 g/L results in decreasing degradation of MB. This is due to non uniform light intensity distribution resulted from overloading. As the result, the reaction rate would be lower with increased photocatalyst dosage. At the same time at lower photocatalyst loading, the degradation of organic molecule (MB) was low, because more light is transmitted through the reactor and lesser transmitted radiation only will be utilized in the photo catalytic reaction (Neppolian *et al.,* 2002). The optimum catalyst dose for synthesized nano-coposite was 0.2 g/L. The result was similar to Xiao *et al.,* (2008) who demonstrated the effect of catalyst loading for the range 0.5 to 4.0 g/L on the solar photo catalytic degradation of MB in the order 1.0 >2.0 > 4 > 0.5 g/L. A number of studies have indicated that the photo catalytic degradation rate initially increased with catalyst loading and then decreases at high values because of light scattering and screening effects. The tendency toward agglomeration (particle-particle interaction) also increases at high solids concentration, resulting in a reduction in catalyst surface area available for light absorption and hence a drop in the photo catalytic degradation rate. Although the number of active sites in solution will increase with catalyst loading, a point appears to be reached where light penetration is to be compromised because of excessive particle concentration. The tradeoff between these two opposing phenomena results in an optimum catalyst loading for the photo catalytic reaction (Adesina, 2004).

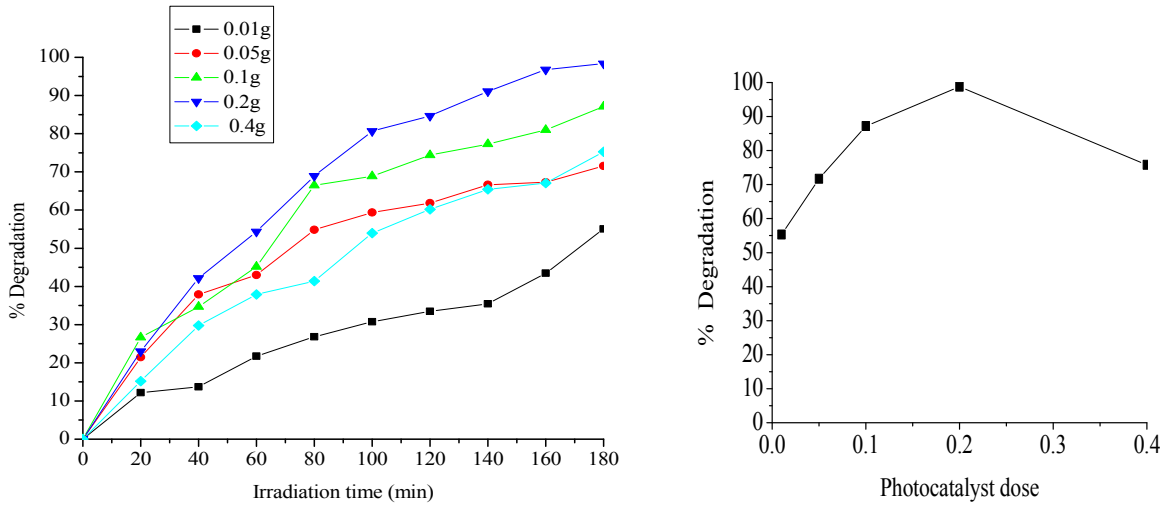

Figure 14. The effect of catalyst loading on photo catalytic activities of as synthesized nano-composite with respect to irradiation time**.**

4.2.3.4. Effect calcination temperature

Calcinations temperature has a vital influence on the optical property, crystal size, and crystal structure of the prepared photocatalyst (Liang *et al.,* 2006). Moreover, the common synthesis of nano photocatalyst usually involves high-temperature calcinations to translate amorphous into crystal structure, which usually results in particle growth and leads to decrease in surface area and decrease in photocatalytic degradation efficiency (Jing *et al*., 2013). Shi *et al.,* (2009) reported that the absorption profile shifted slightly to longer wavelengths (red-shift) with the increase of calcined temperature.

The CdS/ZnO/Ag_3PO_4 nano-composites with different calcinations temperature was used to find the optimum temperature for calination of the as-synthesized nano-composite. This was studied at temperature range between 300^{o}C to 600^{o}C. It was found that a slight increasing of degradation in both calcinations temperature as irradiation time increases but nano-composite calcined at 300^{o}C shows the highest photoactivity. This is due to increase in nanocomposite crystallite size with increasing calcination temperatures which lead to decrease number of active sites of photocatalysts for adsorption of the dye molecules (Pardeshi and Patil, 2009). The photocatalytic degradation efficiency of nano-composite prepared in different calcination

temperature was indicated in the (Figure 15). It shows that the photocatalytic activity of nano-composite was decreasing when calination temperature increases from 300°C to 600°C. The temperature for calination of prepared nano-composite was attained at 300°C for the effective degradation of MB.

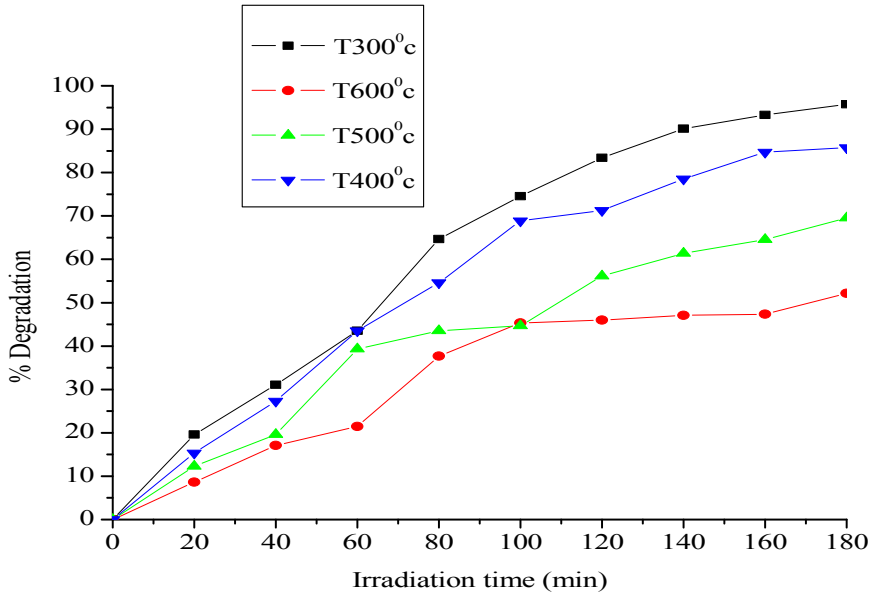

Figure 15. Effect of calcination temperature on the photocatalytic degradation of as-synthesized Nano-composite as function of irradiation time

4.2.3.5. Effect of irradiation time

For this study aqueous solution of MB in the presence of as synthesized nanocomposite irradiate with visible light at different time intervals were recorded. The effect of irradiation time for the removal of MB dye by as synthesized Nano-composites was shown in Figure 16. Photocatalytic degradation of MB in aqueous suspensions of the as synthesized nano-composites was performed to evaluate the effect of irradiation time. When the irradiation time interval increase the degradation efficiency also increases. It has been found that with the increasing in irradiation time interval from 5 min to 30 min, percentage of decoloration was increased from 39.15 to 92.87 % for as synthesized nanocomposite. This is attributed to the fact that, as the irradiation time is increased, the dye molecules have enough time to react with the catalysts and form

hydroxyl radicals which accelerate photocatalytic decoloration reaction and hence percentage of decoloration increases (Daneshvar *et al.,* 2003).

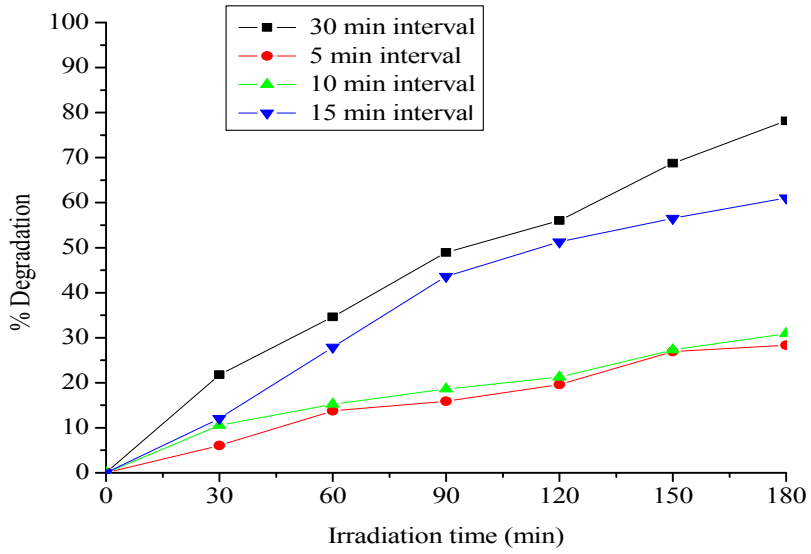

Figure 16. Effect of irradiation time on photocatalytic degradation of as-synthesized nano-composite under visible light irradiation

4.2.3.7. Effect of zeolite loading

In order to investigate the effect of the support loading on photocatalyst two ratio of photocatalyst to zeolite (60:40 and 70:30) respectively was prepared in the first synthesis procedure. Figure.17. revealed that photocatalyst contained a higher amount of zeolite was showed higher photo catalytic activity. Particularly in case of photocatalyst 60:40 ratio supported with zeolite after 160 min photo catalytic degradation tends decrease this is might be due to methylene blue was completely degraded with in160 min. The probable reasons for the apparent photo activity decrease as photocatalyst loading increases in the zeolite (70:30) which may be due to the aggregation of photocatalyst particles in the zeolite cavity or at the external surface and may be due to the blocking of the pores of the zeolites which decrease the adsorption of methylene blue onto the catalyst and as photocatalyst concentration increase, the penetration of the higher-intensity light (lower wavelengths) decrease resulting in reduction in photo activity as photocatalyst concentration increased(figure 17). Similar results were reported by (Xu and Langford, 1997) where in at low loading of titanium oxide on ZSM5 zeolite maximum photo

catalytic activity was observed for the decomposition of chlorophenol. The lowest photo catalytic activity among the TiO_2-coated catalysts was obtained for hither w% TiO_2-coated zeolite photocatalysts.

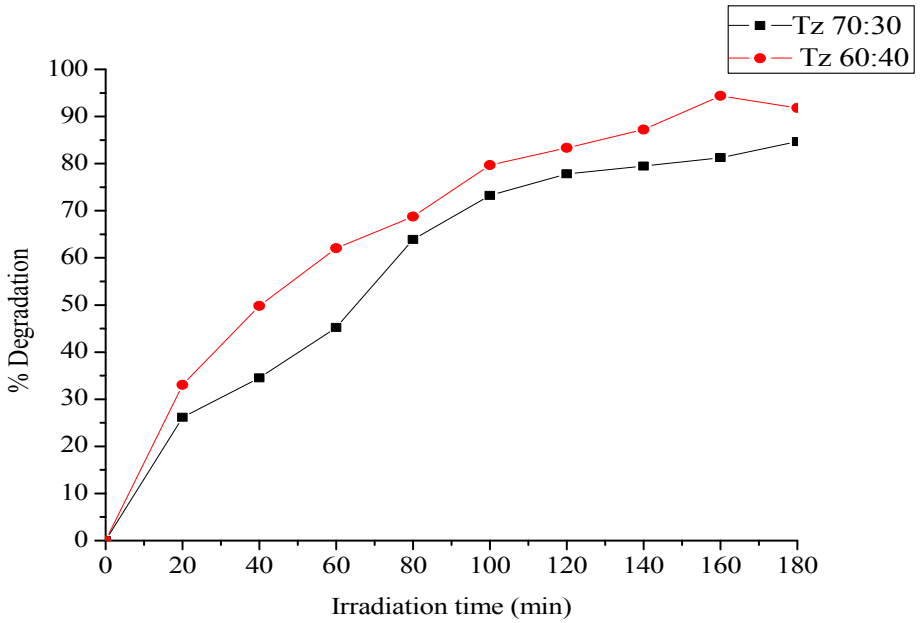

Figure 17. Effect of zeolite loading in photocatalyst on the photo catalytic degradation of MB.

4.2.3.8. Effect of light on the photocatalytic degradation

To test the effect of visible light on photocatalytic degradation of MB, experiments were set up, including photolysis of MB under visible (blank), zeolite under visible light, zeolite supported (Tz) under visible light, zeolite supported (Tz) in dark and naked ternary nanocomposite(T2) under visible light. The samples of dye solution for photolysis experiment and the performance of the bare zeolite under visible irradiation were conducted in the absence of the photocatalyst. The degradation of MB under these conditions provided degradation efficiency of 6.01 and7.09 % respectively (Figure 18). Percent adsorption of MB dyes without light irradiation over Tz was 9.71% (Figure18). It is because of the electron in valence band did not get sufficient excitation energy from the conduction band in order to proceed photocatalytic reaction. In fact for the dark, no electron-hole pair could be generated in semiconducting material without light irradiation. The formation of electron-hole pair is liable for enhancing the redox reaction within

MB dye. That is why the efficiency is low attributed only to adsorption of the dye on the photocatalyst surface.

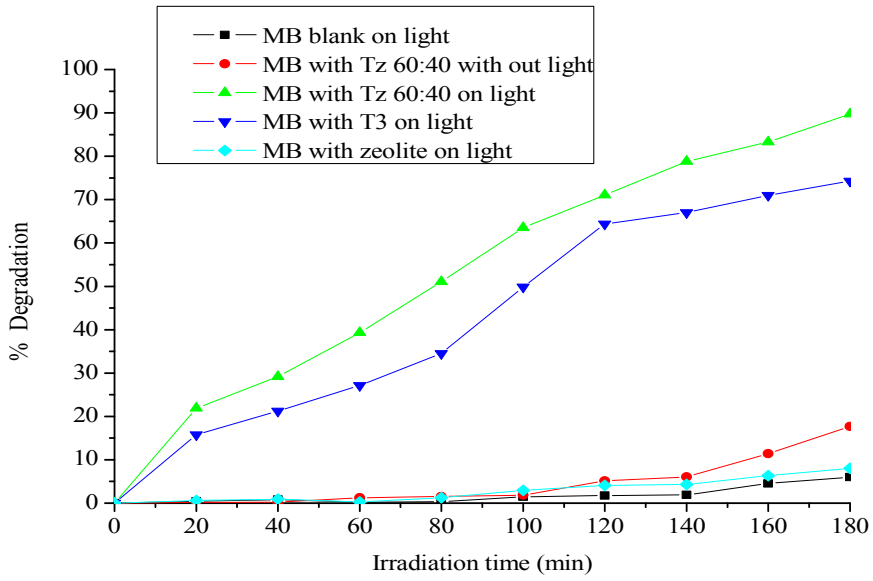

Figure 18. Effect of visible light in photo catalytic degradation of dye (MB) Enhancement as a function of irradiation time with photocatalyst loading 0.2 g/L, dye conc.10 mg/L, at pH 8

The photocatalytic degradation efficiency of the supported composite is higher than the unsupported one under visible light irradiation. The maximum degradation efficiency of Tz and T2 under visible light was 89.75 and 74.27 % respectively. The higher surface area of zeolite favors the adsorption of more water molecules, hydroxyl ions and dye molecules, thus leading to higher photoreactivity. Furthermore, the strong electrostatic field present in the zeolite framework can effectively separate the e- and h+ produced during photo excitation of the ZnO and so resulted in lower recombination of them and higher photodegradation efficiency as compared to the naked ternary nano composite T2.The result of photocatalytic degradation of MB with each experiment is shown in Figure 18.

4.3. Recyclability of Photocatalyst

The photocatalyst stability has a very important role in large scale applications in environmental processes in the treatment of waste water containing different dye pollutants. The reusability of as synthesized nano-composite was performed in four consecutive trials by recovering the photocatalyst in between runs by centrifuging and decanting. For each new recycle the photocatalyst.

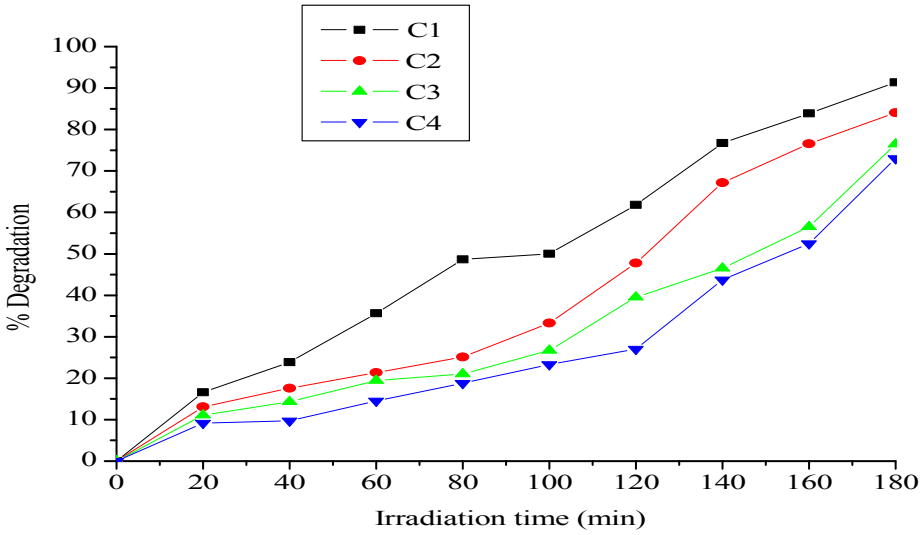

Figure 19. Cyclic runs showing the percentage photocatalytic degradation of MB as a function of irradiationtime Where, C_1, C_2, C_3 and C_4 are first, second, third and fourth cyclic run respectively .

was reused for the degradation of a fresh MB solution under similar condition after photocatalyst sample was filtered and dried. The separation of the reaction mixtures and catalyst was done by decantation.The decoloration rates of MB solution catalyzed by the photocatalysts was sharply decreased after fourth run with the efficiency of the photocatalyst dropping by 18.36 % as compared to the original (Figure 19). This shows that there is reasonably lower leaching of the photocatalyst after performing the experiments. Hence supporting or immobilizing photocatalyst with mesoporous materials such as zeolite promote the application of photocatalysts in the treatment of waste water.

4.4. Analysis of Real Sample

The efficiency of the as-synthesized Tz photocatalyst was studied on the degradation of the real sample under visible light irradiation by using 0.2 g/L photocatalyst loading at pH = 8; the result was shown in Figure 20. Due to the complexity of the wastewater which includes not only mixture of organic dyes but also other chemicals from the bleaching steps (Kiros Guesh *et al.,* 2016) the degradation efficiency in the real wastewater sample (73.24%) was found to be lower than that of model MB solution (92.57%). The photo catalytic tests conducted above indicate that in cases of model MB solution and real wastewater sample, the specific photo catalytic activity is enhanced.

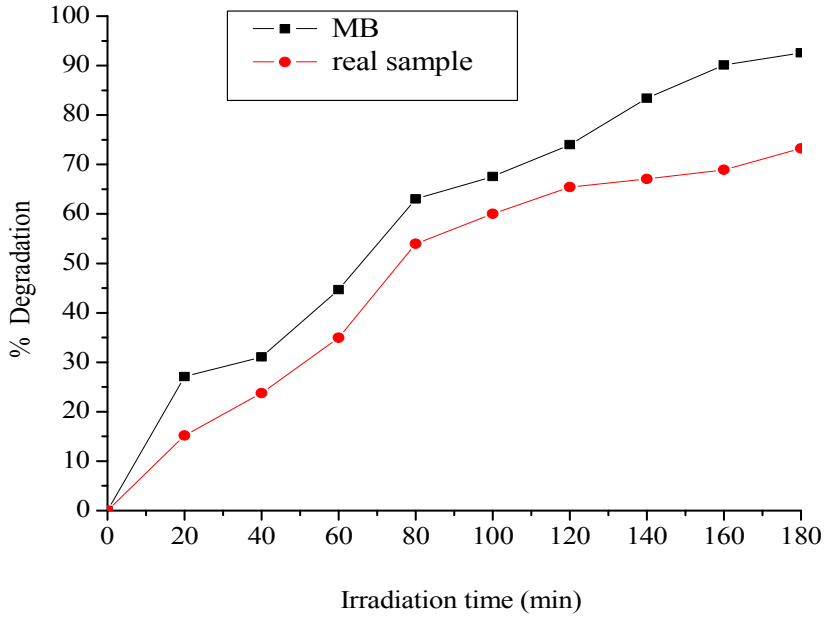

Figure 20. Photocatalytic degradation of MB and real textile wastewater using Tz 60:40

This may be due to the presence of smaller and even less crystalline as-synthesized nano-particles dispersed on the zeolite surface which evidenced from the SEM image of the zeolite loaded nano-composite.

5. SUMMARY, CONCLUSIONS AND RECOMMENDATION

5.1. Summary and Conclusions

The study was aimed to evaluate the potential of zeolite immobilized ternary Nano-composite for photocatalytic wastewater treatment. The single, binary and ternary Nano-composite synthesized by co precipitation method with aqueous solutions of silver nitrate Zinc nitrate hexahydrate , disodiumhydrodgen phosphate , cadimium sulphateoctahydrated and sodium sulfide ,and Zeolite supported ternary Nano-composite material was prepared by impregnation method with dissolving the metal precursors separately in DI water, then the metal containing solution was added in to catalyst support solution. The precipitate formed from the reaction between the two solutions was allowed to settle down for 24 h, then filtered and washed three times each with DI water and ethanol. Then catalyst was dried in an oven for 24 h at 100^0 C. The crystal structures, band gaps, surface morpology, and compositions of all Nano-composites were studied using XRD, UV vis, SEM, AAS, FTIR and PL respectively.The study was examined in detail the effect of key parameters, such as catalysts loading, pH, conc.of dye, calicination temperature, irradiation time, stability, support loading for the degradation of MB dye under UV-Vis light irradiation. Photocatalytic degradation activities of the Nano-composites under visible light irradiation have been evaluated for model pollutant MB dye solution as well as on real sewage sample collected from Hawassa Textile Industry. Results suggested that the zeolite supported $CdS/ZnO/Ag_3PO_4$ nanocomposite photocatalyst exhibited a relatively higher efficiency on the degradation of both MB and real sewage sample which are about 92.57% and 73.24 % respectively. The improved photo degradation efficiency in the visible region of the supported composite could be due to the adsorption characteristics of the zeolite material.

We have prepared zeolite supported $CdS/ZnO/Ag_3PO_4$ hybride system which is effective in photocatalytic degradation of both the model pollutants and real textile west water. On top the role of zeolites is in enhancing the adsorption capacity, in this work we showed that zeolite do have dual role (suppressing electron hole recombination and increasing adsorption capacity) in enhancing photocatalytic activity of $CdS/ZnO/Ag_3PO_4$ hydride system which was evidenced from Photolumensce (PL) study. In generally the result shows that the prepared zeolite supported ternary Nano-composite have presented potential application in wastewater treatment.

5.2. Recommendation

Based on the present study further researcher should be taken into account in future:

Since there is only a few work on the synthesis of zeolite supported ternary nanocomposite, more emphasis in this area is required.

Synthesis zeolite supported CdS/ZnO/Ag_3PO_4 photocatalyst material for new applications such as solar cells, biosensor, and antimicrobial activities.

Study effect of parameters such as intensity of light on the photocatalytic degradation of organic pollutants using zeolite supported CdS/ZnO/Ag_3PO_4.

Characterize TEM, BET in order to determine morphology and specific surface area.

6. REFERENCE

Adesina.2004. Industrial exploitation of photocatalysis: progress, perspectives and prospects. *Catalysis Surveys from Asia,* 8(4): 265-273.

Ahmed, E., Khalid, N.R., Hong, L. and Sana, M. 2010. Preparation and Photocatalysis of Schlumbergera bridgesii-Like CdS Modified One-Dimensional TiO_2 Nanowires on Zeolite. *Journal of Physics Condensed Matter Reviews*, 22 (64): 409–413.

Aksu. 2005. The colored effluents damage the aesthetic quality of water and reduce light penetration and photosynthesis. Process Biochemistry, 40 (3-4): 997-1026.

Alebel, Nibret, Yadav, O.P., Isabel, Diaz, and Abi, Taddesse. M. 2015. Cr-N Co-doped ZnO Nanoparticles:Synthesis, Characterization and Photocatalytic Activity for Degradation of Thymol Blue. *Bulletin Chemical Society Ethiopia*. 29(2): 247-258.

Alireza, Khataee., Reza, Darvishi., Cheshmeh, Soltani., Atefeh, Karimi., Sang .andWoo, Joo. 2015. *Ultrasonics Sono chemistry*, (23): 219–230.

Anandan, S. and Yoon**,** M. 2003. Photo catalytic activities of the nano-sized TiO_2 supported Y-zeolites. *Journal of Photochemistry and Photobiology*, 14(1): 2313-4402.

Anjaneyulu, N., Sreedhara., Chary, D.and Suman, Raji. 2005. Decolourization of Industrial effluents availablemethods and emerging technologies. *Review of Environmental Science,* 4(4): 245-273.

Ansari, S.A., Khan, M.M., Ansari, M.O., Lee, J.and Cho, M.H. 2013. *Journal of Physical Chemistry,* (117): 27023–27030.

Ari, Y. and Sparks, D.L. 2001. *Journal ofcolloid and interface science*, (241): 317-326.

Averyard, R., Binks, B.P.and Clint, J.H. 2005. Emulsions stabilized solely by colloidal particles. *Advanced Colloid Interface Science,* (100): 503–546.

Bahnemann, J. 2004. Photo catalytic water treatment: solar energy applications. *Solar Energy*, 77(5): 445–459.

Bai, J., Li, J., Liu, Y., Zhou, B. and Cai, W. 2010. A new glass substrate photo electro catalytic electrode for efficient visible-light hydrogen production:CdS sensitizedTiO_2 nano tub arrays. *Applied Catalysis* B, *Environmental*, 95(3): 408–413.

Bercoff, H.R., Bertorello, C., Saux, L.B., Pierella, P.M., Botta, Toshiyuki, K., Ying, M. and Zhang, J. 2009. *Journal of Materials science,* 3813-3820.

Bessekhouad, N., Chaoui, M., Trzpit, N., Ghazzal, D., Robert, J.V. and Weber, K.2006. *Journal of Photochemistry and Photobiology* A: *Chemistry,* 183(1): 218-224.

Bi, Y., Ouyang,S.,cao, J and Ye, J. 2011. Facile synthesis of rhombic dodecahedral hetrocryal withenhanced photocatalytic properties and stabilities.Journalof Physical Chemistry, (13): 10071-10075.

Cao J., B.D. Luo, H.L. Lin, B. Xu, S. Chen. 2012. Aluminum salt slag characterization and utilization. Review article, *Journal of Hazardous Materials*, (217–218): 1-458.

Caruso, M. 2001. Antonietti, Sol-gel nano coating: an approach to the preparation of structured materials. *Chemistry of Materials*, 13(10): 3272–3282.

Catalkaya, F. and Kargi. 2007. Color, and removals from pulp mill effluent by advanced processes: A comparative study. *Journals of Hazardous Materials,* 139 (2): 244-253.

Chakrabarti, S. and Dutta, B. 2004. Photo catalytic degradation of model textile dye in wastewater using ZnO as semiconductor catalyst. *Journal of Hazardous Materials* B,112(3):269-278.

Chatterjee, D., and Dasgupta, S. 2005. Anovel visible light-driven photocatalyst film, MoS_2/Ag/TiO_2, was synthesized on a glass-fiber. *Photochemistry Reviews*, 6(2-3): 186-205.

Chauhan, M., Kumar, R.,Umar, A., Chauhan, S.and Kumar,G.2011.Utilization of ZnO nano for photocatalytic degradation of acridine orange. *Journal of NanoScience and technology,* 11(5): 4061-4066.

Chen, C., Xie, Y., Ali, G., Yoo., S.H. and Cho, S.O. 2011. Improved conversion efficiency of CdS quantum dots sensitized TiO_2 nanotube array using ZnO energybarrierlayer.

Chen, S. andLia,L. 2003.Preparation and characterization of nano crystalline zinc oxide by a novel solvothermal oxidation route.*Journal of Crystalline Growth*,152(1-3):184-189.

Chen, S.S. and Mao, L.M. 2007.Titanium dioxide nonmaterial:synthesis properties,modification and applications. *Chemical Reviews,* 107 (7): 2891–2959.

Chen, W. and Lu, W. 2008. Synthesis of photocatalyst containing anatase phase is more efficient than rutile only. *Surface Science Review*, (63): 515-582.

Chiang,Y. and Lin, C. 2013. "Photocatalytic decolorization of methylene blue in aqueous solutions using coupled ZnO/SnO_2 photocatalysts." *Powder Technology,* (246):137–143.

Chiou, C.H., Wu, C. and Juang, R. 2008. Influence of operating parameters on photocatalytic degradation of phenol in UV/TiO_2 process. *Journals of Chemical Engineering* (139): 322–329.

Chira, R., Bhattacharjee, D . and Abhijit, N. 2011. *Physical Science Technology,* (7): 122.

Constapel, M., Schellentrager, M.M. and Gab, S.2009. Degradation of reactive dyes in wastewater from the textile industry by ozone: analysis of the products by accurate masses.*Water Resource Review*, (43):733-743.

Corma, A. and Garcia, H. 2004."Zeolite-based photocatalysts." *Chemical Community,*43-59.

Corrent, S., Cosa, G., Scaiano, J. C., Galletero, M. S., Alvaro, M. and Garcia, H.2001."Intrazeolite properties of nanosized TiO_2 clusters included in zeoiltes Y,beta, and mordenite." *Chemistry of Materials,* (13): 715-722.

Curridal, M. , Comparelli, R., Cozzli, P., Mascolo, G. and Agostiano, A. 2003. Colloidal oxide nano particles for the photo catalytic degradation of organic dye. *Material Science Engineering* C, (23): 285-289.

Daneshvar, N., Salari, D., Khataee, A.R. 2003. Photocatalytic degradation of azo dye acid red14 in water: investigation of the effect of operational parameters. *Journal of Photo chemistry and Photobiology,* A*: Chemistry,* 157(1): 111–116.

Dong, W., Zhijie, L., Bo, H.,·Yao, X. and Yuhan S. 2006. Hydrothermal synthesis**,** the photocatalytic activity of the silica-modified TiO_2 sample held good photo catalytic activity. *Journal of Colloid and Interface Science ,(*282): 109-119.

Dutta, P. K. and Severance, M. 2011. "Photoelectron transfer in zeolite cages and its relevance to solar energy conversion." *Journal of Physical Chemistry Letter,* (2): 467-476.

Elahifard, M.,Rahimnejad, S., Haghighi, S. and Gholami, M. 2007. AgBr/TiO_2 Visible light Photo catalyst for destruction of bacteria. *Journal of American Chemical Society,*1(29): 9552-955.

Ewais, E.M. and Geassy, K.2008.In-siut synthesis of magnetic Mn-Zn ferrite ceramic objects by solid state reaction. *Australian Ceramics, (*44): 57-62.

Fotou,G. and Pratsinis,S.1996.Photocatalytic destruction of phenol and salicylic acid with aerosol-made andcommercial titanium powders.*Journal of Chemical Engineering* (6): 237-251.

Gaya, A.and Abdullah,M. 2008.Heterogeneous photo catalyticdegradation of organic contaminant over titanium dioxide: a review of fundamentals, progress and problems. *Journal of Photo chemistry and Photobiology C, Photochemistry Reviews*, 9(1):1–12.

Gerven, T.V., Mulc, G., Moulijn, J. and Stankiewicz, A.2007. A review of intensification of photo catalytic processes. *Chemical Engineering Process,* (46):781–789.

Gogate, P. and Pandit,A. 2004. Areview of imperative technologies forwastewater treatmentII: hybrid methods. *Advanced Environmental Research*, 8 (3-4):501-551.

Gomes, E., Fernandes, J. and Lima. 2005. Fluorescence probes used for detection of reactive oxygen species. *Journal of Bio chemistry Biophysics Methods*, 65 (2-3): 45-51.

Haileyesus,Tedla. Isabel, Díaz.,Tesfahun, Kebede.and Abi, Taddesse.M.2015.Synthesis,characterization and photocatalytic activity of zeolite supported $ZnO/Fe_2O_3/MnO_2$ nanocomposites. *Journal of Environmental Chemical Engineering*, (3):1586–1591.

Han, Q., Kuang, M.S., Jin, Z.X., Xie, L.S. and Zheng, R. 2009. Synthesis of titania nano sheets with a high percentage of exposed (001) facets and related photo catalytic properties. *Journal of the American Chemical Society,* (113): 3152-3153.

Hashimoto, S. 2003. "Zeolite photochemistry: impact of zeolites on photo chemistry and feed back from photochemistry to zeolite science."*Journal of Photochemistry Photobiology* ,C (4): 19-49.

He,H., Hung.L., Cao, and J. *2010*. photodegradiation of methyl orange aqueous on $MnWO_4$ powder under different lightbresources and intial pH. *Desalination, (*252): 149-159.

Hermann, J.M., Disdier, J. and Pichat, P.J. 1986. *Journal of Physical Chemistry,*(90):6028–6034.

Hisanaga, T. and Tanaka, K. 2002.Photo catalytic degradation of benzene on zeolite incorporated TiO_2 film. *Journal of Hazardous Materials*, (93): 331-337.

Hoffmann, S.T., Martin, W.Y., Choi, D.W. Bahnemann. 1989. *Journal of Photochemical. A: Chemistry*, (50) , 103-105.

Hong, R.Y., Pan, T.T., Qian, J.Z. and Li, H. Z. 2006. Synthesis and surface modification of ZnO nanoparticles. *Chemical Engineering Journal,* 119(2-3): 71-81.

Hong, R.Y., Li, J.H., Chen, L.L., Liu, D.Q., Li, H.Z., Zheng, Y. and Ding, J. 2009. *Powder Technology,* (189): 426.

Hong. X.,Wu.Q. Zhang, M.Xiao ,G.Yang,M.Qiu,G. 1999. Hydro apatite supported Ag_3PO_4 nano particles with higher visible photo catalytic Activity. *Journal of Applied Catalysis,* 258 (2012): 4801-480.

Houas, H., Lachheb, M., Ksibi, E., Elaloui, C.,Guillard, J. and Cao, P. 2011. Anew perspectivefor effect of Bi on the photo catalytic activity of Bi doped TiO_2. Applieed catalysis B:*Journal of Environmental Science*, (125):294-303.

Huang, M., Xu, C., Wu, Z., Huang, Y., Lin, J.and Wu, J. 2008. Photo catalytic discolorization of methyl orange solution by Pt modified TiO_2 loaded on natural zeolite. *Dyes Pigment,* (77): 327-34.

Huang, J.,Cui,Y.and Wang, X.2010.Visible light sensitive ZnGe oxy nitride catalystdecomposition of organic pollutants in water. *Environmental Science Technology,* (44):3500–3504.

Jana, TK., Pal A, Chatterjee K. 2014. Self assembled flower like CdS–ZnO nanocomposite and its photocatalytic activity. *Journal of Alloys Compound,* (583): 510–515.

Jang Y. J., Simer, C. and Ohm, T. 2010. Comparison of zinc oxide nanoparticles and its nanocrystalline particles on the photocatalytic degradation of methylene blue. *Material Resource,* (41): 67-77.

Janitabar-Darzi, S. and Mahjoub, A.R. 2009. Investigation of phase transformations andphoto catalytic properties of sol-gel prepared nanostructured ZnO/TiO_2 composites. *Journal of Alloys Compound*, (486): 805–808.

Jing, J., Feng, J., Li, W. and Yu,W. 2013."Low temperature synthesis of water-dispersible anatase titanium dioxide nanoparticles for photocatalysis."*Journal of Colloid and InterfaceScience,* (396): 90–94.

Kamat, P.V., Prashant,V., SaidBarazzouk, S.and GeorgeThomas, K. 2002. Fluorophore-Gold Nano assembly. *Journal of Physical Chemistry*, (106): 18-21.

Kamat, P.1993.Photo physical, photo chemical and photo catalytic aspects of metal nanoparticles. *Chemical Engineering Review*, (93): 267-300.

Kamigaito, O., Moore, D.R., Sato, N., Kurauchi, T.and Sato, S**.**1991. Fatigue of thermoplastic composites, in thermoplastic technology and engineering. *Journal of Materials Science ,(*26): 3891-3898.

Kiros, Guesh., Alvaro, Mayoral., Carlos, M.arquez., Alvarez., Yonas, Chebude. And Isabel, Díaz. 2016. Enhanced photocatalytic activity of TiO_2 supported on zeolites tested in real waste waters from the textile industry of Ethiopia. *Journal of Microporous and Mesoporous Materials,* (225): 88-97.

Kim, M.C., Joo, D.J., Shin, W.S., Choi, J.H., Choi, S.J., Han, M.H. and Ha, T.W. 2006. Decolorization of reactive dyes', for textile effluent coagulation. *Journal of Hazardous Materials Water Research*, 40 (3): 435–444.

Kim, Y.and Yoon, M. 2001. TiO_2/Y-Zeolite encapsulating intramolecular charge transfer molecules: A new photocatalyst for photoreduction of methyl orange in aqueous medium. *Journal of Molecular Catalyst* A Chemistry, (168):257-263.

Kim, H., Kim, J., Kim, W. and Choi,W.2011.Enhanced photo catalytic and photo electrochemicals activity in the ternary hybrid of $CdS/TiO_2/WO_3$ through the cascadal electrontransfer. *Journal of Physical Chemistry* C, (115): 9797–9805.

Komarneni, S. and Katsuki, H. 2002.Nano phase materials by a novel micro wave hydro thermal Process. *Pure and Applied Chemistry*, (74): 1537-1543.

Kurien, S., Sebastian, S., Mathew, J. and George, K. C. 2004 "Structural and electrical properties of nano-sized magnesium aluminate." *Indian Journal of Pure and Applied Physics,* 42, (12): 926–933.

Kwon, Y., Kim, K., Lim, C. and Shim, K. 2002.Characterization of ZnO nano powders synthesized by the polymerized complex method via organo chemicalroute."*Journal of Ceramic Processing Research,* 3, (3):146–149.

Lavand, A. B.and Malghe,Y.S. 2015. *Advanced Materials Lett*er, (6): 695.

Lee, T., Akhtar, M.and Park,D.2012.Water splitting on Rhodamie B dye sensitized Co-doped TiO_2 catalyst under visible light. *Applied catalysis* B, *Environmental,* 397–401.

Lee *et al*., 2005. Novel Ag3PO4/TiO2 composites for efficient decomposition of gaseous 2-propanol under visible-light irradiation. *Catalysis Communications.*

Li, A. and Wu,W.2003.Synthesis of mono dispersed ZnO nano particles and their luminescent pro perties. *Journal of Engineering Materials*, (9):75-87.

Li, F. S., Sun, S., Jiang, Y., Xia, M., Sun, M. and Xue, B. 2008. "Photo degradation of an azo dye using immobilized nanoparticles of TiO_2 supported by natural porous mineral." *Journal of Hazardous Materials,* 152(3):1037–1044.

Liang, C., Hou, M., Zhou, S. 2006."The effect of erbium on the adsorption and photo degradation of orangeI in aqueous Er^{3+} TiO_2 suspension." *Journal of Hazardous Material,* 138 (3): 471–478.

Lin, C. , Lu,Y., Hsieh, C. and Chien, S. 2009. Surface modification of highly orderedTiO_2 nano tube arrays for efficient photo electro catalytic water splitting. *Journal of Applied Physical chemistry* C, (115): 9320-9334.

Lin, H.M., Tzeng, S.J., Hsiau, P.J. and Tsai,W.1998. Electrode effects on gas sensing properties of nano crystalline zinc oxide. *Nanostructure Materials,* 10(3): 465-477.

Liu,Y., Su, G., Zhang, B., Jiang,G. andYan, B.2011.Nano particle based strategies for detection and remediation of environmental pollutants. Analyst, (136): 872–877.

Liu, X.and Chen, Z.2008. Avisible light response TiO_2 photocatalyst realized by catatonicsdoping and its application for phenol degradation. *Journal Hazardous Materials,*(152):48-55.

Liu, S., Sun, H., Liu, S. and Wang, S. 2013."Graphene facilitated visible light photodegradation of methylene blue over titanium dioxide photocatalysts."*Chemical Engineering Journal,* (214): 298–303.

Lucas, M., Tavares, P.and Peres, J.2013."Photo catalytic degradation of Reactive Black5 with TiO_2-coated magnetic nano particles." *Catalysis Today,* (209):116–121.

Marquez, F., Marti,V.,Palomares, E.and Garcia, H.2002.Observation of azo chromophore fluorescence and phosphorescence emissions from DBH by appling exclusively the orbital confinement effect in siliceous zeolites devoid of charge balancing cat ions. *Journal of American Chemical Society,* (124): 7264-7265.

Mishra, V., Chakravadhanula,V. and Hrkacetal, K.2012. Crystal growth behavior of Au/ZnO nano composite under different annealing environments and photo switch bility.*Journal of Applied Physics*, (116):12462-12467.

Mohammad, Reza.,Mostafa, Fazli.and Mohammad, Hossein.2015. Decomposition of organicche micals by zeolite TiO_2 nano composite supported onto low densitypolyethylene filmunder powered by solar radiation. *Applied Catalysis* B*:Environmental,* (183): 407–416.

Neppolian, B., Choi, H., Sakthivel, S., Arabindoo, B. and Murugesan,V. 2002. "Solar-induced photo catalytic degradation of three commercial textile dyes."*Journal of Hazardous Materials,* 89 (2-3): 303–317.

Obare, S.O., Meyer**,** G. 2004.TiO_2 has also been extensively studied for oxidative or reductive removal of organic pollutants. *Journal of Environmental Science and Health a toxic Hazard Substances Environmental Engineering*, 39 (10): 2549–821.

Ouyang, J.,Wei, L., Mingliang,Wang. C. and Shifu, C. 2011. Ag_3PO_4/ZnO: An efficient visible

light sensitized composite with its application in photo catalytic degradation of Rhodamine B . *Materials Research Bulletin*, (48): 106–113.

Pandey, A., R.K. Chakrabarty, L., Liu, and M.I. Mishchenko, 2015. Empirical relationships between optical properties and equivalent diameters of fractal soot aggregates at 550nm wavelength. *Optics Express Research* 23: (24) 1354-1362.

Pardeshi, S., Patil, A.2009.Effect of morphologyand crystallite size on solar photocatalytic activity zinc oxide synthesized by solution free mechano chemical method.*Journal of Molecular Catalysis*A: *Chemical*, (308): 32–40.

Paré, B. 2011. Synthesis of the photocatalyst**.** All chemicals were reagent grade and used without further purification. *Journal of Physical Chemistry* C, (115): 8064–8071.

Pawar, R C.and Lee, C.S. 2013. *Applied Catalysis B*, (144): 57.

Qi, Xiao., Jiang, Zhang., Chong., Xiao. and Xiaoke, Tan. 2008. Photo catalytic degradation of methylene blue over Co_3O_4/Bi_2WO_6 composite under visible light irradiation. *Catalysis Community,* (9): 1247–1253.

Qi, Xiao., Qitao, Zhou., Jiang, Zhang. and Linli, Ouyang. 2009. Photo catalytic decolorization of methylene blue over monoclinic pyrochlore type $Pb_2Nb_2O_7$ under visible light irradiation. *Journal of Alloy Compound*, (468): 9–12.

Qiu, X., Fang, Z., Liang, B., Gu, F. and Xu, Z. 2011. "Degradation of decabromodiphenyl ether by nano zero-valent iron immobilized in mesoporous silica microspheres." *Journal of Hazardous Materials,* (193):70–81.

Rajabi, J., Tayade, Ramchandra,G. andKulkarni, J.2013.Enhanced Photo catalytic Activity of TiO_2 -Coated NaY and HY-Zeolites for the degradation of methylene Blue inWater . *Engineering Chemical Research***, (**46): 369-376.

Rawal,S.B., Bera,S., Lee, D., Jang, D.J., and Lee,W.I.2013. Design of visible-light photocatalysts by coupling of narrow band gap semiconductors and TiO_2: effect of their relative energy band positions on the photocatalytic efficiency*Catalysis Science and Technology,* (3):1822–1830.

Robison, A., Caballero, M.,Villegas, C., Moure, P., Durán, J. and Fernández, F. 2001.Controlled Precipitation methods: formation mechanism of ZnO nano particle. *Journal of the European Ceramic Society,* 21 (7): 925–930.

Rosari, Saleh., Nadia,Febiana. Djaja. 2014.UV-light photo catalytic degradation of organic dyes with Fe-doped ZnO nanoparticles. *Superlattices and Microstructures*, (74): 217–233.

Saravanan, R., Karthikeyan, N.,Gupta,V., Thangadurai, P.,Narayanan,V. and Stephen, A.2013. *Materials Science Engneering,* (33): 2235–2244.

Shah, A.H., Manikandan, E., Basheer, M. and Ganesan, V.2013. "Enhancedbioactivity of Ag/ZnO nanorods -A comparative antibacterial Study." *Journal of Nano medicine and technology,* 4, (3):2–6.

Shankar, M.V., Anandan, S., Venkatachalam, N., Arabindoo, B., Murugesan, V. 2006. Fine route for an efficient removal of 2, 4-dichlorophenoxyacetic acid (2, 4-D) by zeolite-supported TiO_2. *Chemosphere,* (63): 1014-21.

Shao, R., Sun, L., Tang, L. and Chen, Z. 2013. "Preparation and characterization of magnetic core-shell $ZnFe_2O_4$@ZnO nanoparticles and their application for the photodegradation of methylene blue." *Chemical Engineering Journal,* (217):185–191.

Shih, P.Y. 2004.*Materials chemistry and physics*, (84):151-156.

Silva, C.G.and Faria, J. 2009. Effect of key operational parameters on the photo catalytic oxidation of phenol by nano crystalline sol-gel TiO_2 under Uv-irradiation. *Journal of Molecular Catal ysis* A, *Chemistry,* (305):147–154.

Silva, R. F. and Zaniquelli, M. E. 2002."Morphology of nanometric size particulate aluminium-doped zinc oxide films." *Colloids and Surfaces* A, (198–200): 551–558.

Sohrabnezhad, S., Pourahmad, A. and Radaee, E.2009."Photo catalytic degradation of basic blue 9 by CoS nanoparticles supported on AlMCM-41 material as acatalyst." *Journal of Hazardous Materials,* 170 (1): 184–190.

Sowbhagya and Sannaiah, Ananda. 2014. *American Chemical Science Journal,* (4): 616-637.

Starosud, A., Bhargava, A., Langford, C. H. and Kantzas, A.1999."Development of new photo catalytic method and reactor for wastewater treatment."*Study of Surfac Science Cataly sis,* (122): 219-228.

Tai,C., Gu, H., Zou, H. and Guo, Q. 2002. Anew simple and sensitive fluorometric method for the determination of hydroxyl radical and its application. *Journal of Chemical Society*, (58): 661-667.

Tang, Junwang., Zhigang, Zou .and Jinhua, Ye.1997. Kinetics of MB degradation and effect of pH on thephotocatalytic activity of MIn_2O_4 (M = Ca, Sr, Ba)under visible light irradiation. *Research on Chemical Intermediates ,* 31 (4–6): 513–519

Takeuchi, M., Tsujimaru, K., Sakamoto, K., Matsuoka, M.andYamashita, H. 2003. Effect of Pt loading on the photo catalytic reactivity of titanium oxide thin films prepared by ion engineering techniques.*Research Chemistry Intermediates*, (29): 619-29.

Tao,Y.,Wu,C.andMazyck, D.2006.Removal of methanol from pulp and paper mills using combine activated carbon adsorption and photo catalytic regeneration.*Chemosphere,*(65): 35-42.

Teja, A.S., Holm, L.J. and Sun. Y.P. 2002. Production of magnetic oxide nanoparticles, supercritical fluid technology in materials science and engineering: synthesis. Properties and Applications. *Material Science and Engineering Research*, (41): 1873-1876.

Ushio, M., Miyayama, H.andYanagida,T.1994.Effects of interface states on gas sensing Properties of CuO/ZnO thin-film hetero junction. *Sensors and Actuators B*, 17(3): 221–226.

Vinod, K., Gupta, Rajeev, Jain, Alok, Mittal., Shilpi, Agarwal. and Shalini, Sikarwar.2012. *Materials Science Engnreening* C, (32):12–17.

Vu, T., Río, L.,Valdés Solís, T. and Marbán, G.2013."Stainless steel wire mesh supported ZnO for the catalytic photo degradation of methylene blue under ultraviolet irradiation." *Journal of Hazardous Materials,* (246-247):126–134.

Wahab, R., Kim, Y. S., Lee, K.and Shin, H. S.2013. *Journal of Material Science*, (45): 2967.

Walter, E.L., Warren, J.R., McKone, S.W., Boettcher, Q.X., Mi, E.A., Santori,N.S and Lewis, S.R . 2010. Solar water splitting cells. *Chemical Reviews*, (110): 6446 - 6473.

Wang, J., Ren, F., Yi, R., Yan, A., Qiu, G. and Liu, X. 2009. Solvothermal synthesis and magnetic properties of size-controlled nickel ferrite nanoparticles. *Journal of Alloys Compounds,* (479): 791-796.

Wang X., Hu Z., Chen Y., Zhao G., Liu Y., Wen Z. 2002. A novel approach towards high performance composite photocatalyst of TiO2 deposited on activated carbon. *Applied Surface Science*, (255): 3953–3958.

Weber,E.J. and Adams, R.L.1995. Chemical and sediment-mediated reduction of the azo dye dispersed Blue79. *Environmental Science and Technology*, (29): 1163-1170.

Xi, D.L. and Li, Y. 2004. Development of a bioreactor for remediation of textile effluent and dye mixture: a plant-bacterial. *Journal of Environmental Science Pollute Review*,11(6): 372-377.

Xiang, Q.,Yu, J. and Jaroniec, M. 2012. Graphene based Semiconductor photocatalysts. *Chemical Society Reviews,* (41): 782–796.

Xiao, Q., Zhang, J., Xiao, C., Si, Z.and Tan, X.2008. Solar photo catalytic degradation of methyle ne blue in carbon-doped TiO_2 nanoparticles suspension. *Solar Energy*, (82):706-713.

Xu, Y. and Langford, C. H.1997. Photo activity of titanium dioxide supported on MCM41, zeolite X, and zeolite Y. *Journal of Physical Chemistry* B, *(*101): 3115-3121.

Xu, J. Q., Pan, Q.Y., Shun, Y.A. and Tian, Z.Z. 2000. Grain size control and gas sensing properties of ZnO gas sensor. *Sense Actuator B, Chemistry*, (66): 277-279.

Xu, Z. and Yu, J. 2011.Visible-light-induced photo electrochemical behaviors of Fe-modified TiO_2 nanotube arrays. Article Note, (3): 3138–3144.

Yao, W.F. , , Xu, X.H. , Wang, H., Zhou, J.T., Yang, X.N. , Zhang, Y. , Shang, S.X. and Huang, B.B. 2004. Photocatalytic property of perovskite bismuth titanate. *Applied Catalyst,* B: *Environmental,* (52): 109–116.

Yang, H.T., Fu, A.B., Yu, X.C. and Jiang, L. 2012. Large surface mesoporous TiO_2 nanopartcles: Synthesis, growth and photo catalytic performance. *Journal of the Colloid and Interface Science,* (355): 312-320.

Yang, G., Yang, B., Xiao, T.and Yan, Z.2013. *Applied Surface Science,* (283):402.

Yang, X., F., Ma, K., Li, Y., Guo, J., Hu, Li, W., Huo, M. and Guo, Y. 2008. Mixed phase titania Nanocomposite codoped with metallic silver and vanadium oxide: New efficient photocatalyst for dye degradation. *Journal of Hazard. Mater.* (175): 429–438.

Yu, J., Zhao, X.and Zhao, Q. 2000. Effect of surface structure on photocatalytic activity of TiO_2 thin films prepared by sol–gel method. Thin Solid Films, (379):7–14.

Zhang,C., Zhou, X.and Lin, D.S.2010.Synthesis of clay minerals. *Applied ClayScience,* (50):1–11.

Zhang, Y., Chen, C., Zhan, Y., Lin,, Zheng Q., Wei, K and. Zhu. J. 2008. *Journal of Physical Chemistry C,* (112):10773–10777.

Zhao,C.,Chen,W.and Ma,Y.2005. Photo catalytic degradation of organic pollutants undervisible li ght irradiation. *Topics in Catalysis*, (35): 269–278.

Zhao, L., Chen, X.,Wang, X., Zhang,Y.,Wei,W., Sun,Y., Antoinette, M. and Titirici, M. M. 2010. One step solvothermalm synthesis of acarbonTiO_2 dyade structure effectively promoting visible light photocatalysis. *Advanced Materials,* (22): 3317–3321.

Zhao, L., Jiang, Q.and Lian, J.2008.Visible light photo catalytic activity of nitrogen doped TiO_2 in film prepared by pulsed laser deposition. *Applied Surface Science,* (254): 4620-4625.

Zhong, X.,Yuan, D., Junfeng, C. and Xin, X. 2012. Photo catalytic process for properties, and appl ications of nanosized photocatalytic materials as transparent photocatalysts. *Article*, (8): 930-950.

Zhou, W., Liu, H., Wang, J., Liu, D., Du, G. and Cui, J. 2010. Ag_2O/TiO_2 Nano belts Hetero structure with enhanced ultraviolet and visible photo catalytic activity. *Applied Materials Interfaces,*(2): 2385–2392.

Zou, S.W., Lim, S.F, Zheng, Y.M, Chen, J.P .2013. Dye removal from aqueous solution. *Environmental Science Technology,* (42): 2551–2556.

7. Appendix

7.1.Appendix figures

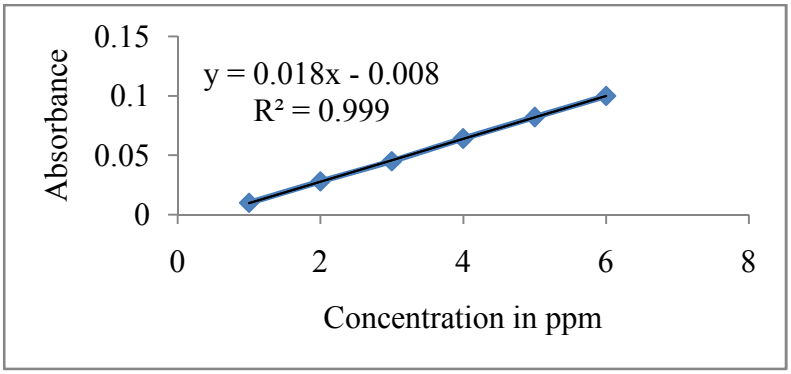

Appendix figure 1.Calibration curve for Ag

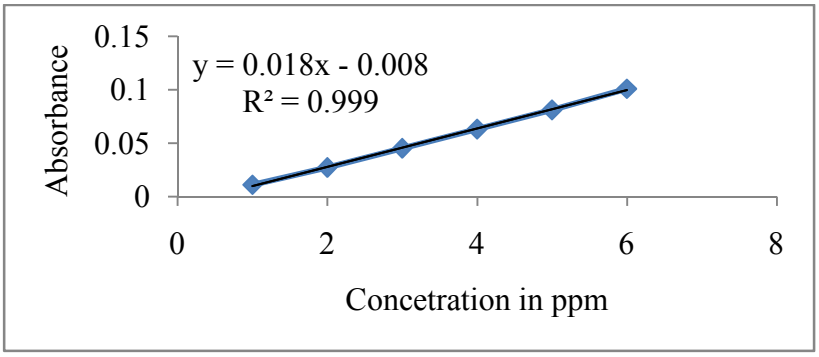

Appendix figure 2.calibration curve for Zn

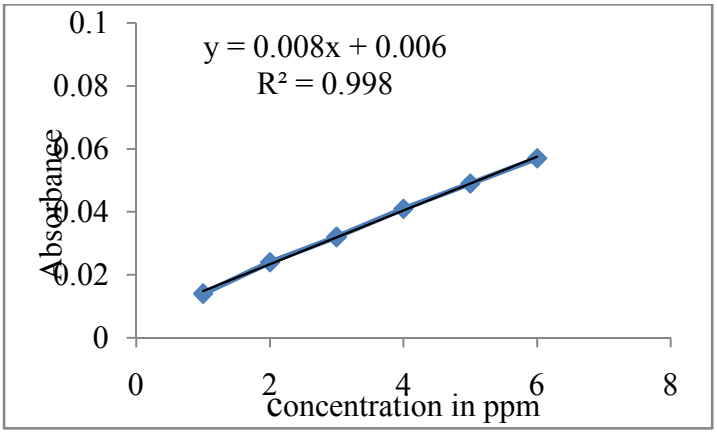

Appendix figure 3.calibration curve for Cd

7.2.Appendix Tables

AppendixTable 1. AAS readout for Ag

1ppm	0.010
2ppm	0.028
3ppm	0.045
4ppm	0.064
5ppm	0.082
6ppm	0.100

Appendix Table 2. AAS readout for Zn

1ppm	0.011
2ppm	0.026
3ppm	0.044
4ppm	0.063
5ppm	0.081
6ppm	0.101

Appendix Table 3. AAS readout for Cd

1ppm	0.014
2ppm	0.024
3ppm	0.032
4ppm	0.041
5ppm	0.049
6ppm	0.057

Appendix Table 4. The elemental analysis from EDS of as-sythensized nano-composite of T2

Element	Weight %
Phosphorus	4.6
Sulfur	10.9
Zinc	59.0
Silver	12.7
Cadmium	12.8

Appendix Table 5. The elemental analysis from EDS of as-sythensized nano-composite of Tz 60:40

Element	Weight %
Aluminum	0.9
Silicon	2.2
Phosphorus	2.7
Sulfur	8.1
Zinc	59.5
Silver	10.3
Cadmium	16.3

Appendix Table 6. Comparisons of Photocatalytic degradation of synthesized single, binary and ternary nano-composite

Time	S1	S2	S3	B1	B2	T1	T2	T3	T4
0	0	0	0	0	0	0	0	0	0
20	3.05	5.17	4.2	7.93	5.41	9.4	8.78	6.08	4.13
40	7.13	7.37	4.9	13.51	4.13	20.12	20.9	13.9	9.07
60	7.87	11.45	9.29	16.04	13.57	27.81	26.27	19.62	12.57
80	8.8	15.13	12.67	18.83	14.04	32.07	34.47	24.74	17.4
100	12.8	16.43	13.29	19.44	17.28	33.96	38.65	30.92	18.00
120	12.8	21.61	16.28	22.49	17.74	45.83	49.86	39.15	23.69
140	15.57	26.14	17.32	22.66	21.33	47.16	58.82	39.98	27.29
160	17.23	33.92	19.55	25.54	23.23	53.22	63.17	41.21	31.19
180	22.11	45.02	26.1	29.78	28	61.87	69.1	43.31	36.21

Appendix Table 7. Comparison of photocatalytic activity of zeolite supported and unsupported nano-composites

Time	T1 % degr.	T2 % degr.	T3 % degr.	T4 % degr.	Tz60:40
0	0	0	0	0	0
20	9.4	8.78	6.08	4.13	33.33
40	20.12	20.9	13.9	9.07	51.82
60	27.81	26.27	19.62	12.57	62.05
80	32.07	34.47	24.74	17.4	68.75
100	33.96	38.65	30.92	18	79.68
120	45.83	49.86	39.15	23.69	83.33
140	47.16	58.82	39.98	27.29	89.32
160	53.22	63.17	41.21	31.19	96.87
180	61.87	69.1	43.31	36.21	94.79

Appendix Table 8. The effect of pH on the photocatalytic activities of as-synthesized nano-composites

Time	pH 4	pH 12	pH 8	pH10	pH 6	pH 2
0	0	0	0	0	0	0
20	16.6	22.21	24.82	23.64	19.73	15.24
40	21.04	27.26	36.19	35.4	22.65	20.09
60	32.72	39.48	56.11	48.22	36.91	26.5
80	37.13	44.87	68.55	51.58	42.29	30.14
100	45.54	53.35	72.02	59.14	49.58	37.06
120	57.28	64.35	85.02	67.23	59.56	41.66
140	69.28	76.38	96.51	79.26	71.77	56.66
160	78.27	81.96	93.07	89.06	79.79	69.01

Appendix Table 9.The photocatalytic activity of as-synthesized nano-composites as effect of initial dyes concentration

Time	10 ppm	15 ppm	20 ppm	25 ppm	30 ppm
0	0	0	0	0	0
20	16.33	12.34	9.33	10.22	2.97
40	27.07	19.42	17.5	15.76	10.52
60	33.33	30.96	24.61	19.85	18.62
80	51.82	55.23	42.56	27.91	21.23
100	68.75	61.92	52.51	33.51	28.36
120	79.68	73.22	64.55	39.90	29.16
140	81.25	77.82	70.13	42.33	33.68
160	83.33	79.49	76.69	51.82	47.68
180	89.32	83.68	79.21	68.75	50.80

Appendix Table 10.The percentage photocatalytic activity of as-synthesized nano-composites as effect of photocatalyst loading

Time	0.01 g/L	0.05 g/L	0.1 g/L	0.2 g/L	0.4 g/L
0	0	0	0	0	0
20	12.17	21.47	26.64	22.98	15.19
40	13.69	37.9	34.7	22.17	29.74
60	21.73	42.98	45.17	54.33	37.9
80	26.8	54.85	66.49	68.95	41.39
100	30.76	59.37	68.86	80.64	53.97
120	33.47	61.83	74.4	84.67	60.2
140	35.43	66.62	77.3	91.12	65.43
160	43.47	67.27	81	96.77	67.04
180	55.03	71.543	87.11	98.38	75.24

Appendix Table 11. Comparison of photocatalytic activities of as-synthesized nano-composites at different calcination temperature

Time	300^0 C	600^0 C	500^0 C	400^0 C
0	0	0	0	0
20	19.59	8.64	12.30	15.33
40	31.09	17.09	19.59	27.33
60	43.51	21.44	39.33	43.51
80	64.66	37.66	43.51	54.62
100	74.55	45.33	44.66	68.85
120	83.39	46.01	56.16	71.25
140	90.11	47.1	61.39	78.51
160	93.28	47.33	64.55	84.71
180	95.75	52.13	69.55	85.72

Appendix Table12. Effect of irradiation time on photocatalytic decoloration of MB dye under UV-vis light irradiation

Time	30 min	5 min	10 min	15 min
0	0	0	0	0
30	21.78	6.08	10.52	12.08
60	34.64	13.76	15.23	27.92
90	48.92	15.9	18.62	43.66
120	56.05	19.62	21.23	51.28
150	68.75	26.94	27.33	56.55
180	78.15	28.36	30.92	61.07
210	84.37	29.16	41.17	67.31
240	87.11	30.03	49.86	71.12
270	93.75	33.51	51.43	74.25
300	96.87	39.15	63.71	79.32

Appendix Table 13.The cyclic runs showing the percentage photo catalytic degradation of MB as a function of irradiation time

Time	C1	C3	C2	C4
0	0	0	0	0
20	16.62	11.07	13.11	9.17
40	23.87	14.30	17.58	9.73
60	35.64	19.47	21.23	14.51
80	48.64	21.02	25.12	18.78
100	50.03	26.71	33.30	23.31
120	61.82	39.52	47.81	27.05
140	76.74	46.53	67.19	43.75
160	83.91	56.54	76.57	52.5
180	91.38	76.46	84.06	73.02

Appendix Table 14. Effect of zeolite loading on the photo catalytic degradation of MB.

Time	Tz 60:40	Tz 70:30
0	0	0
20	33.04	26.16
40	49.82	34.52
60	62.05	45.23
80	68.75	63.92
100	79.61	69.22
120	83.33	74.82
140	87.22	79.49
160	94.37	81.25
180	91.15	84.68

Appendix Table 15. Effect of visible light on the photocatalytic Degradation of dye (MB) Enhancement

Irradiation time	MB blank on light	Tz dark	Tz on light	T3 on light
0	0	0	0	0
20	0.43	0.172	21.89	15.76
40	0.84	0.194	29.17	21.23
60	0.22	1.263	39.33	27.17
80	0.338	1.554	51.09	34.49
100	1.46	1.84	63.51	49.87
120	1.77	5.11	71.07	64.4
140	1.9	6.07	78.8	67.03
160	4.52	11.41	83.28	71.
180	6.01	17.71	89.75	74.27

Appendix Table16. Percentage photocatalytic degradation of real textile wastewater and MB using Tz 60:40

Time	% MB in Tz 60:40	% real sample in Tz 60:40
0	0	0
20	27.11	15.19
40	31.09	23.74
60	44.66	34.93
80	63.03	53.97
100	67.55	60.02
120	74.021	65.43
140	83.39	67.04
160	90.1	68.95
180	92.57	73.24